University of Tartu

Faculty of Science and Technology

Tartu Observatory

Ave Ansper

SENTINEL-2/MSI APPLICATIONS FOR EUROPEAN UNION WATER FRAMEWORK DIRECTIVE REPORTING PURPOSES

Master thesis (30 EAP)

Supervisors: PhD Krista Alikas (TO, UT)

PhD Piia Post (UT)

Allowed to defense:

Supervisor:

Supervisor:

Head of the department:

TARTU 2018

Sentinel-2/MSI applications for European Union Water Framework Directive reporting purposes

The European Parliament and The Council of the European Union have been established the Water Framework Directive (2000/60/EC) (WFD) for all European Union member states to achieve at least "good" ecological status of water evenly in all European waters, which are larger than 50 hectares. European Space Agency satellite Sentinel-2/MSI (S2/MSI) has suitable 10, 20, 60 m spatial resolution to monitor Estonian lakes as required by the WFD. The aim of the master thesis is to analyze the suitability of S2/MSI data to monitor water quality in inland and coastal waters. This consists of two steps, firstly to test various atmospheric correction (AC) processors to remove the influence of atmosphere and secondly, to compare and develop chlorophyll-a (chl-a) algorithms to estimate ecological status of water by chl-a in Estonian lakes. The study showed, that S2/MSI is suitable for estimating chl-a in water, showing the spatial and temporal dynamics in the lakes. However, ACs are sensitive to surrounding lands and often fail in narrow and small lakes. Due to that, developing and validating chl-a algorithms is not possible in every case, but initial results show S2/MSI could be really valuable source of information for fulfilling WFD monitoring requirements.

Keywords: European Union Water Framework Directive (2000/60/EC), ecological status of water, chlorophyll-a, Sentinel-2/MSI, Copernicus, remote sensing

CERCS: T181 Remote sensing

Sentinel-2/MSI võimalused Euroopa Liidu veepoliitika raamdirektiivi rakendusteks

Euroopa Liidu Parlament ja Euroopa Liidu Nõukogu on kehtestanud veepoliitika raamdirektiivi (WFD) kõigile Euroopa Liidu liikmesriikidele, et saavutada vähemalt "hea" vee ökoloogilise seisundi klass kõigis Euroopa vetes, mis on suuremad kui 50 hektarit. Euroopa Kosmoseagentuuri satelliidil Sentinel-2/MSI (S2/MSI) on sobiv ruumiline lahutus 10, 20, 60 meetrit, mis võimaldab seirata WFD nõuete kohaselt Eesti järvi. Magistritöö eesmärgiks on analüüsida S2/MSI sobivust veekvaliteedi seireks järvedel ning rannikualadel. Magistritöö koosneb kahest osast, kus esmalt testiti erinevaid atmosfäärikorrektsiooni protsessoreid, et eemaldada atmosfääri segav mõju ning teiseks

võrreldi ning arendati klorofüll-a (chl-a) algoritme, et hinnata Eesti järvede vee ökoloogilise seisundi klassi chl-a järgi. Magistritöö käigus selgus, et S2/MSI on võimeline hindama kanalite asetusest lähtudes chl-a kontsentratsiooni vees, näidates ruumilist ja ajalist dünaamikat järvedes. Siiski, atmosfäärikorrektsioonid on liiga tundlikud ümbritsevale maapinnale ning ei anna tulemusi kitsaste ning väikeste järvede puhul. Seetõttu ei ole chl-a algoritmide arendamine ja valideerimine võimalik kõikidel juhtudel, kuid esialgsed tulemused näitavad, et S2/MSI omab potentsiaali, et olla informatsiooniallikaks WFD seirenõuete täitmisel.

Märksõnad: Euroopa Liidu veepoliitika raamdirektiiv (2000/60/EC), vee ökoloogiline seisund, klorofüll-a, Sentinel-2/MSI, Kopernikus, kaugseire

CERCS: T181 Kaugseire

CONTENTS

INTRODUCTION

The European Parliament and The Council of the European Union have been established the Water Framework Directive (2000/60/EC) (WFD) for all European Union (EU) member states to implement water management evenly in all European waters. The Directive obligates to estimate ecological status in waterbodies, through monitoring and classification, where the water surface area is 50 hectares (ha) or larger (Ferreira *et al.* 2007, Ministry of Environment, Regulations 2009). According to the WFD, phytoplankton is one of the important biological element for estimating the ecological status of water. The amount of phytoplankton in water is estimated by measuring quantity of chlorophyll-a (chl-a), which is the pigment of phytoplankton (Dörnhöfer *et al.* 2017).

Regular monitoring is time consuming, whereas the lack of finances and the accessibility to waterbodies (due to the land or property rights) restrict the monitoring capabilities. Remote sensing is one opportunity to support regular monitoring with high temporal and spatial frequency (Dörnhöfer and Oppelt 2016). Copernicus program provides long-term monitoring from the space through Sentinel missions, which started with the launch of Sentinel-1A/SAR in 2014. Sentinel-2/MSI (S2A/MSI) is part of the Sentinel mission and gives advantages over other ocean color satellites with its high spatial resolution (Klein *et al* 2017), although the spectral and radiometric resolution are optimized for monitoring vegetation. The first S2/MSI satellite was launched in 2015 and by the continuation of the mission (S2B, S2C, S2D), it is expected to systematically provide long-term data at least until 2031 (Krebs 2017) or even longer with second generation of S2 satellites.

The objective of this study is to analyze the suitability of the S2/MSI data for estimating water quality parameters in lakes, which gives advantages over regular monitoring and thereby estimate ecological status of lakes according to the WFD. The first part of this study is to compare different atmospheric correction (AC) processors over Estonian lakes, because approximately 90% of the signal measured by the sensor originates from the atmosphere (scattering by molecules and aerosols) (Shanmugam 2012), and find the best AC processor based on the results of comparing *in situ* measurements and S2/MSI data. As the chl-a is the key parameter of biological elements, secondly, the objective is to find chl-a algorithms for different water types, that will be applicable to S2/MSI data.

1. Literature overview

1.1. European Union Water Framework Directive

The aim of the Water Framework Directive is to achieve at least "good" ecological status of inland and coastal waters by using program of measures and maintain status "good" if it already exists (European Commission 2000). EU member states have to implement through the water policy regular monitoring to estimate ecological status in waterbodies (Ferreira *et al.* 2007). The classification of ecological status is divided into five categories: "very good", "good", "moderate", "bad", "very bad". Water ecological status "good" indicates very light bias due to human activity from reference conditions (Ministry of Environment, Regulations 2009). Biological indicators represent phytoplankton, where chlorophyll is one part of phytoplankton and describes the phytoplankton abundance, aquatic flora, benthic invertebrate and fish fauna. Hydromorphological elements such as hydrological regime indicates water flow dynamics and morphological conditions describe depth fluctuations. In physico-chemical elements water transparency, thermal conditions, oxygenation, state of nutrients and acidification status are monitored (Munne and Prat 2006).

According to the EU WFD regulations, 89 lakes should be monitored regularly in Estonia (Figure 1), which are divided into 8 different groups by the type of waterbody (Table 1). Estonian small lakes belong into Type 1 to Type 5 group, two biggest lakes Peipsi and Võrtsjärv both form its own group and coastal lakes belong to Type 8. To determine ecological status of lakes, then water samples of phytoplankton and physico-chemical elements are collected from May to September, except in Peipsi and Võrtsjärv. Water samples of Peipsi are collected from April to October, although percent of Cyanobacteria from total phytoplankton biomass are calculated only for period from July to September. In Võrtsjärv, water samples are collected only from July and August and biomass of diatoms is only based on the results of September (Ministry of Environment, Regulations 2009).

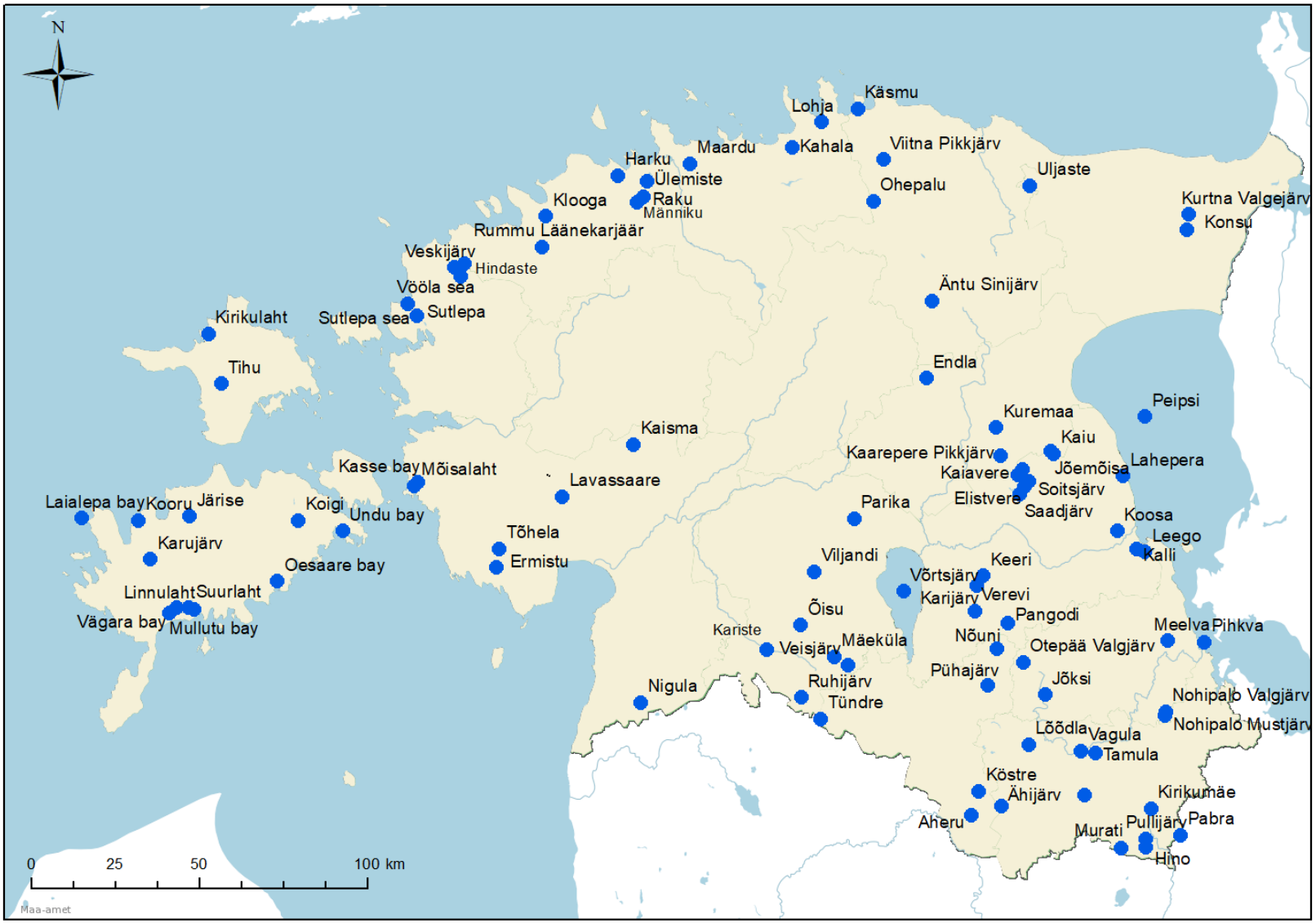

Figure 1. According to the EU WFD, 89 lakes of Estonia, larger than 50 ha, which should be monitored regularly (Ministry of Environment, Regulations 2009; basemap: Maa-amet, 2018)

Table 1. Classification of waterbodies based on the EU WFD regulations (Ministry of Environment, Regulations 2009)

Type of lake	Water surface area	Stratification	Water color	Amount of chloride	pH	Number of lakes
Type 1	<10 km^2	Non-stratified	Dark/light	Low	Hard	1
Type 2	<10 km^2	Non-stratified	Dark/light	Low	Moderate	33
Type 3	<10 km^2	Stratified	Dark/light	Low	Moderate	21
Type 4	<10 km^2	Non-stratified	Dark	Low	Soft	10
Type 5	<10 km^2	Non-stratified	Light	Low	Soft	8
Type 6 (Võrtsjärv)	100-300 km^2	Non-stratified	Light	Low	Moderate	1
Type 7 (Peipsi and Lämmijärv)	>1000 km^2	Non-stratified	Light	Low	Moderate	2
Type 8	Coastal lakes	Non-stratified/ stratified	Dark/light	High	Hard/ Moderate/ Soft	13

Every indicator of ecological status (biological, physico-chemical and hydromorphological) have been associated with certain thresholds to assign ecological status of water. Therefore ecological status of a lake is a combined result of each quality indicator and type specific conditions that should be considered. Type specific thresholds for chl-a are showed on the Table 2. To estimate the ecological status of water, then at least seven quality parameters should be considered, therefore all the parameters are equally important (Ministry of Environment, Regulations 2009).

Table 2. Thresholds for chl-a (mg/m^3) estimating ecological status of for different lake types (Ministry of Environment, Regulations 2009)

Type of lake	Very good	Good	Moderate	Bad	Very bad
Type 1	<1	1-2	>2-3	>3-5	>5
Type 2	<10.8	10.8-28	>28-52	>52-215	>215
Type 3	<5.8	>5.8-13	>13-26	>26-104	>104
Type 4	<10	10-20	>20-30	>30	>30
Type 5	<5.4	5.4-13	>13-26	>26-103	>103
Type 6	≤24	>24-38	>38-45	>45-51	>51
Type 7	≤3 (Peipsi), ≤6 (Lämmijärv and Pihkva)	>3-8 (Peipsi), >6-13 (Lämmijärv and Pihkva)	>8-20 (Peipsi), >13-37 (Lämmijärv and Pihkva)	>20-38 (Peipsi), >37-75 (Lämmijärv and Pihkva)	>38 (Peipsi , >75 (Lämmijärv and Pihkva)
Type 8	<5	5–15	>15–25	>25	>25

1.2. Deriving information from satellite data

For fulfilling EU WFD, consistent monitoring is essential for estimating water quality in lakes. Since 1970s the use of remote sensing technologies has increased because of successful satellite missions (Chen *et al.* 2007, Matthews 2011, Salem *et al.* 2017a). Advantages over traditional monitoring methods are temporal and spatial coverage (Matthews 2011, Salem *et al.* 2017b) and the possibility to estimate water quality in non-accessible waterbodies (Matthews 2011, Lins *et al*. 2017). Remote sensing gives the possibility to observe waterbodies from local to global range and to estimate water quality regularly (Chen *et al.* 2004). However, remote sensing is depending on weather conditions, because optical sensors are sensitive to clouds and air mass changes. Not only the wide coverage is a major advantage, also historical data plays an important role, because of the possibility to compose time series (Werdell *et al*. 2018).

The EU's Copernicus Program provides full and free access for quality controlled data and consistent technology improvement, which is seen as an important source of information for

environmental monitoring. These possibilities advance the research based on remote sensing data, which is very valuable for estimating water quality (Klein *et al.* 2017). Satellite images of waterbodies provide an opportunity to derive some of the important parameters of water quality for fulfilling WFD requirements such as chl-a, phytoplankton biomass and transparency (Alikas *et al.* 2015). Chl-a is a pigment of phytoplankton, that indicates the trophic status of water. Through the photosynthesis, the phytoplankton convert CO_2 and H_2O into O_2 and because of this process they are responsible for primary production in water (Matthews 2011, Duan *et al.* 2007). In addition, chl-a is the main indicator of phytoplankton biomass (Moses *et a.l* 2009, Zhang *et al.* 2015, Wozniak *et al.* 2014, Zhang *et al.* 2014) and could be used determine the water clarity (Salem *et al.* 2017b), because phytoplankton blooms cause important environmental problem, such as eutrophication and affect directly inland waters through the water quality and indirectly drinking water, fishing and swimming (Zhang *et al.* 2015). Whereas transparency of water indicates the light field, that penetrates the water and ensure sufficient amount of light for underwater ecosystems (Alikas 2016).

Based on the optical properties, natural waters have been classified into two types in remote sensing applications: Case 1 and Case 2 waters. Case 1 waters are phytoplankton dominated waters and typically represent 'oceanic waters' (Morel & Prieur 1977). Case 2 waters are optically complex waters with different concentrations of optically active substances (OAS) such as chl-a, colored dissolved organic matter (CDOM) and total suspended matter (TSM). Because of large and independent variations of OAS in Case 2 waters, the estimation of water quality parameters in these conditions are usually more complex than in Case 1 waters (Odermatt *et al.* 2012, Zhang *et al.* 2014). Because of high and independent chl-a, CDOM and TSM, lakes in Estonia represent Case 2 waters.

Different aspects have to be considered while deriving water quality parameters from remote sensing data. As 90% of the signal that reaches back to the sensor is affected by the absorption and scattering by different particles (water vapour, ozone, oxygen, carbon dioxide) and aerosols the correct AC procedure is essential for deriving water quality parameters from lakes. Optical sensors measure reflected light from the atmosphere and the surface of waterbody at visible and near-infrared (NIR) wavelengths. AC processors remove the scattered signal of atmosphere and retrieve signal from the surface of water, called water-leaving reflectance (ρ) (Shanmugam 2012, Matthews 2011). For Case 1 waters, AC assumes that the water-leaving radiance is zero in the NIR part of the spectrum, therefore it does not work in turbid waters because of the scattering by particle that increase the spectrum values

in the NIR part. Additionally problems occur in shallow waters where signal is affected by the bottom reflectance and water-leaving radiance is no longer zero in the NIR part of the spectrum. Therefore it causes over-correction in the visible part of the ρ spectrum (IOCCG 2000). In small and narrow lakes or in the vicinity of the coast, adjacency effect is also influencing reflected light field, because pixels are affected by the signal originating from the surrounding areas (Candiani *et al.* 2007). Pixels from the coastline are brighter than water pixels and due to scattering the values of ρ are higher, which cause AC failures in these pixels. Furthermore, it precludes for deriving important water quality parameters from satellite data, such as chl-a, CDOM and TSM (Sterckx *et al.* 2011).

1.3. Development of chl-a algorithms

There are two main options, for estimating chl-a in remote sensing applications: model-based and empirical approach. Model-based approach is using bio-optical models to simulate ρ or top-of-atmosphere (TOA) radiance spectrum with specified water constituents. More widely used is empirical the approach, which is based on band ratios and therefore has smaller sensitivity, but easier to develop and apply (IOCCG 2000, Matthews *et al.* 2011). As Case 1 waters are phytoplankton dominated waters, where reflected light from water surface is related directly to chl-a, band ratio models that are based on two or three band ratios will work successfully (Moses *et al*. 2009). Most accurate results are obtained using bands at blue-green wavelengths (440-550 nanometers (nm)) because of absorption peak of chl-a at near 440 nm and minimal absorption near 550 nm (Morel and Prieur 1977):

$$chl - a \propto \frac{R(\lambda_{blue})}{R(\lambda_{green})} \quad (1)$$

For Case 2 waters, these algorithms fail because absorption and scattering due to CDOM and TSM (Fell *et al.* 2003). Second chl-a absorption peak, which is around 675 nm, gives a chance to use a band ratio algorithms around this wavelength ($R(\lambda_{red})$ over Case 2 waters (Matthews *et al.* 2010). For optically complex waters with high phytoplankton biomass, the Two-Band algorithm as for Case 1 waters is mostly used, but with the reflectance in the red and in the NIR part of the ρ spectrum (Gitelson 1992):

$$chl - a \propto \frac{R(\lambda_{NIR})}{R(\lambda_{red})} \quad (2)$$

As Case 2 waters are strongly affected by OAS, then wavelength R(λ_{NIR}) may be between 700-720 nm, where absorption of water constituents is minimal or beyond 710 nm, where absorption is dominated by the water and scattered by the water constituents (Lins *et al.* 2017). For turbid waters Three-Band NIR-Red Model algorithm has been developed (Gitelson *et al*. 2003):

$$chl - a \propto \left[\frac{1}{R(\lambda_1)} - \frac{1}{R(\lambda_2)}\right] * R(\lambda_3) \quad (3)$$

where R(λ_1) is maximally sensitive to the absorption peak of chl-a, R(λ_2) is minimally sensitive to the absorption of chl-a and R(λ_3) is minimally affected by the absorption of chl-a (Zimba and Gitelson 2006).

For highly turbid waters Le (2009) has done further development for the Three-Band NIR-Red Model and has added R(λ_4) in the equation. In the Four-Band NIR-Red Model the fourth band should minimize the impact of absorption and backscattering of TSM in R(λ_3) and is located at NIR wavelengths:

$$chl - a \propto \left[\frac{1}{R(\lambda_1)} - \frac{1}{R(\lambda_2)}\right] / \left[\frac{1}{R(\lambda_4)} - \frac{1}{R(\lambda_3)}\right] \quad (4)$$

Additionally various so-called line height algorithms have been developed. For detecting surface blooms and near-surface vegetation in coastal and ocean waters Maximum Chlorophyll Index (MCI) is used for MERIS sensor. It is based on height of the peak at 709 nm which detect effectively blooms in water surface (Gower *et al.* 2008):

$$MCI = L_{709} - L_{681} - \left[\frac{709 - 681}{753 - 681} * (L_{753} - L_{681})\right] \quad (5)$$

where L is TOA radiance at the specific wavelengths. According to Gower (2008) MCI algorithm is used effectively with reflectance values as well, derived from atmospherically corrected images, instead of radiances.

The Flourescenece Line Height (FLH) algorithm is meant for low-biomass waters and it uses the fluorescence peak maximum near 685 nm, that is located between linear baseline of two adjacent bands (Gower 1999):

$$FLH = L_2 - L_1 - (L_3 - L_1) * \frac{(\lambda_2 - \lambda_1)}{(\lambda_3 - \lambda_1)} \quad (6)$$

where L_i is the water-leaving radiance at wavelength λ_i. Band i = 2 assumed to be band for detecting fluorescence and i = 1,3 are the baselines.

1.4. Water remote sensing satellites

The first sensor on satellite Nimbus 7, for monitoring water quality of oceans, was launched in 1978 and was named Coastal Zone Color Scanner (CZCS) (Salem *et al.* 2017a, Yoder *et al.* 1987). Satellite ocean color missions have been continued with different sensors such as Sea-viewing Wide Field-of-view (SeaWiFS), Moderate Resolution Imaging Spectroradiometer (MODIS) and Medium Resolution Imaging Spectrometer (MERIS) (Woerd and Wernand 2015). New generation satellites are launched by European Satellite Agency (ESA) through Sentinel missions. MERIS sensor was the first sensor specifically designed to monitor optically complex waters and was the prototype for the OLCI (Ocean and Land Colour Imager) sensor on Sentinel-3 (S3) platform, that gives opportunity for high quality water monitoring with 300 m spatial resolution (Malenovsky *et al.* 2012). As inland waters are smaller than OLCI spatial resolution, Multi Spectral Instrument (MSI) on Sentinel-2 (S2) satellite gives a chance to monitor smaller waterbodies. Similar sensor to MSI is Operational Land Imager (OLI) onboard Landsat-8 (launched 2013), which, in addition to land data, provides data from aquatic systems as well (Table 3). The spatial resolution of OLI is 30 meters, but temporal resolution of 16 days is not sufficient for regular monitoring. The mission of Landsat started in 1972 with Landsat 1, which was Earth imaging satellite (Mandanici and Bitelli 2016).

Table 3. Comparison of Ocean Color Satellites

	Sentinel-2	Sentinel-3	Landsat-8	Envisat
Sensor	MSI - *Multi-Spectral Imager*	OLCI- *Ocean and Land Colour Imager*	OLI - *Operational Land Imager*	*MERIS - Medium Resolution Imaging Spectrometer*
Operator	ESA	ESA	NASA/USGS	ESA
Mission	Terrestial	Ocean Color	Earth imaging	Ocean Color
Operational time	S2A 2015-... S2B 2017-... S2C planned 2021 S2D planned 202x	S3A 2016-... S3B 2018-... S3C planned 2021 S3D planned 202x	2013-...	2002-2012 not operational
Temporal resolution	2-3 days	2 days	16 days	2-3 days
Spatial resolution	10, 20, 60 m	full resolution at 300 m, reduced resolution at 1200 m	30 m	full resolution at 300 m, reduced resolution at 1160 m
Radiometric resolution	12 bit	16 bit	16 bit	16 bit
Bands	13	21	11	15

The S2 mission is originally meant for monitoring land cover changes and is composed of two identical satellites – S2A was launched in 2015 and S2B in 2017. S2 mission includes satellites S2C and S2D as well, which are planned to be sent to the orbit in the next decade (Table 3). Sensor MSI measures in 13 spectral bands from 443 to 2190 nm with spatial resolution 10, 20, 60 m and the radiometric resolution is 12-bit (Figure 2). As MSI is similar sensor to OLI, but due to the higher revisiting of S2 and more spectral bands in visible and NIR wavelengths, the MSI has advantages over OLI (Pahlevan *et al*. 2017). As OLCI sensor is designed to monitor ocean color from the space, then the positions of the bands are located more on the visible and NIR wavelengths. Also, the Signal-to-Noise Ratio (SNR) is lower in S2/MSI and higher in OLCI. The band of OLCI for deriving chl-a is located in the middle of the second chl-a absorption peak (the centre of the band is 674 nm) and is easily detectable absorption in the water by chl-a (Figure 2). The chl-a absorption band for MSI is wider (width 38 nm) than for the band in OLCI sensor (width 7.5 nm) and might have lower sensitivity to measure the absorption peak at 675 nm compared to OLCI. However, spatial resolution of MSI (starting from 10 m) gives advantage over OLCI (300 m) for monitoring small lakes.

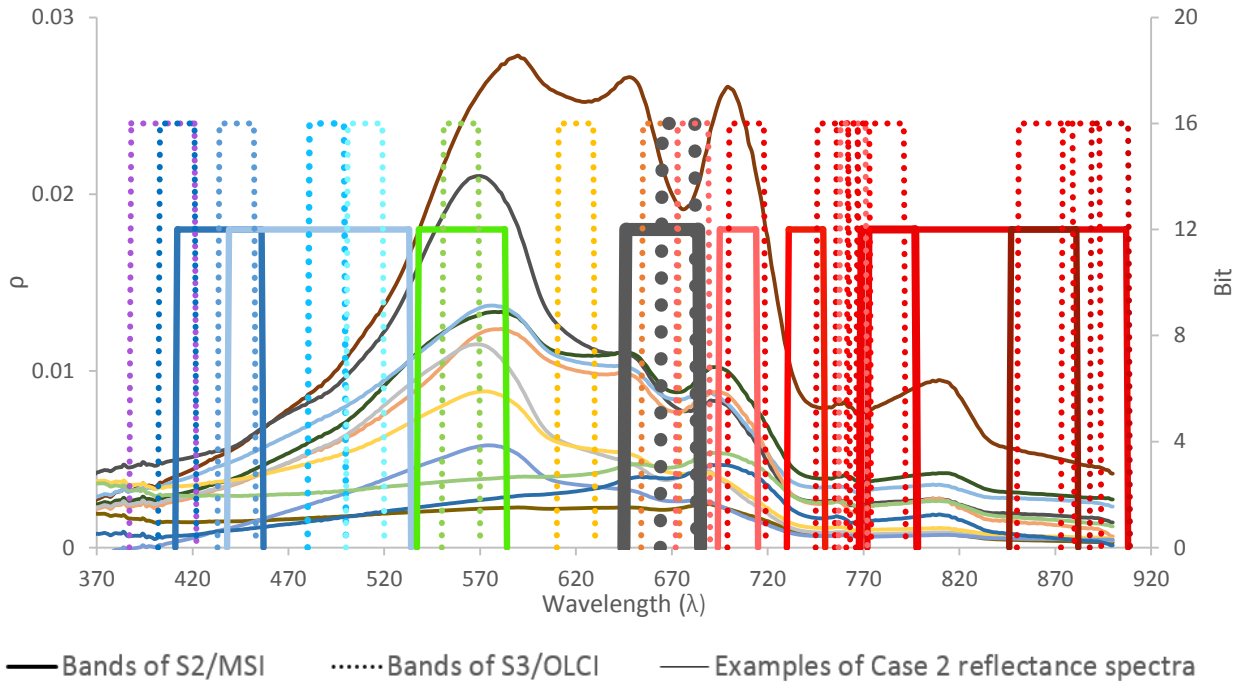

Figure 2. Comparison of MSI and OLCI bands at specific wavelengths (visible and NIR part of the spectrum). Dotted lines are representing the location and width of OLCI's bands and solid lines for MSI. Grey lines are describing chl-a bands at the chl-a absorption peak of both sensor. For understanding the band locations, the different ρ spectrums are added on the figure.

2. Materials and methods

2.1. *In situ* datasets

Radiometric measurements were performed in Estonian lakes and coastal waters from 2015 to 2017 in the same period as S2/MSI has been on an orbit. Above-water TriOS system is measuring upwelling radiance $L_u(\lambda)$, downwelling radiance $L_d(\lambda)$ and downwelling irradiance $E_d(\lambda)$ with three RAMSES spectrometers simultaneously after every 30 seconds (Figure 3). The spectral range of RAMSES starts at 350 nm and the step of measurement is 1 nm. Field measurement protocol and the derivation of water-leaving reflectance is based on the published protocols (Ruddick *et al.* 2006, Tilstone *et al.* 2002).

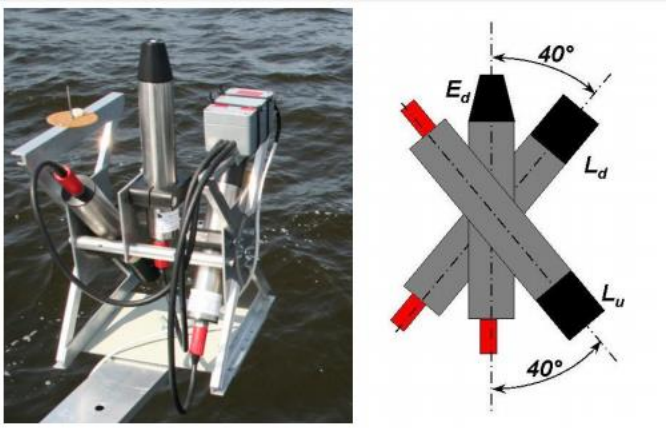

Figure 3. Above-water TriOS system with three RAMSES spectrometers, which are measuring upwelling radiance $L_u(\lambda)$, downwelling radiance $L_d(\lambda)$ and downwelling irradiance $E_d(\lambda)$

The ρ is calculated by equation:

$$\rho(\lambda) = \pi \frac{Lu - \rho Ld}{Ed} \quad (7)$$

where ρ(W) is the sea surface reflectance as function of wind speed W(m/s) is $\rho = 0.0256 + 0.00039W + 0.000034W^2$.

Simultaneously to radiometric measurements, water samples are collected and chl-a (mg/m^3), TSM and full spectrum of IOPs (a_{cdom}, a_{ph}, a_{nap}) are measured. Water samples are collected from the surface layer and kept in the dark and in refrigerator until analyses. Chl-a samples are filtered and pigment extraction is done with 5 ml 96% ethanol and extractions

are kept 6-20 hours at room temperature in dark. Chl-a is measured spectrophotometrically with Hitachi U-3010 (430-750 nm) and the results of chl-a is derived from equation according to Jeffrey and Humphrey (1975):

$$chl - a = \frac{(11.85 * E_{664} - 1.54 * E_{647} - 0.08 * E_{630}) * a}{l = V} \quad (8)$$

where a is an amount of ethanol (mL), V is an amount of filtered water (L) and l is the thickness of the cuvette (cm). From E_{630}, $E6_{47}$ and E_{664} the value at 750 nm (Uudeberg *et al.* 2014).

Chl-a in small lakes is measured by the National monitoring from type specific period from 2015-2017. Water samples are collected from the water surface and are measured by standard of Estonia EVS-ISO 5667-4. The method of measuring chl-a in the laboratory is the same as described in the previous section. Besides water samples, water color, transparency, water temperature, oxygen in water, pH etc. are measured (Eesti Maaülikooli põllumajandus- ja keskkonnainstituut 2016).

2.2. S2/MSI data

S2/MSI data is divided into three different levels by processing type. Level-0 is raw data what is non-accessible for users and is the input for Level-1 data. Level-1 data includes radiometric and geometric corrections with ortho-rectification of TOA reflectance and spatial registration on a global reference system with sub-pixel accuracy. Level-1 product is 10, 20 or 60 m spatial resolution based on the specific band. Level-2 products are higher level products, where AC procedure is applied providing bottom-of-atmosphere (BOA) reflectance (Baillarin *et al.* 2012).

2.2.1. ACOLITE

ACOLITE is AC processor for coastal and inland waters and was developed for Landsat 8/OLI and S2/MSI images. ACOLITE is a tool for high resolution satellites and is able to give results over extremely turbid, narrow and small water bodies. The process of AC includes a Rayleigh correction for scattering air molecules and aerosol correction.

ACOLITE (v20170718.0) performs AC independently of ESA's Sentinel toolbox Sentinel Application Platform (SNAP). Default output is water-leaving reflectances at S2/MSI wavelengths. Different IOP algorithms are optional outputs. After Rayleigh correction only water pixels are presented and non-water pixels such as land, clouds, glint etc. are removed (Vanhellemont and Ruddick 2016).

2.2.2. C2RCC

C2RCC previously known as Case 2 Regional CoastColour processor is developed for optically complex Case 2 waters. The C2RCC processor uses a large database of simulated ρ and TOA radiances. It is based on the neural network technology which has trained on extreme ranges of scattering and absorption properties.

C2RCC v0.15 is available through SNAP. It is applicable to previous and current water remote sensing satellites such as S2/MSI. Output products are ρ, inherent optical properties, chlorophyll, TSM and CDOM. Before applying AC there is possibility to add inputs for salinity (salinity of inland waters = 0.0001), elevation, ozone, temperature, air pressure. For estimating weather and atmosphere parameters European Centre for Medium-Range Weather Forecasts (EMCWF) source was used. For quality check pixels named VALID_PE (the operators valid pixel expression has resolved to true) and RHOW_OOR (one of the inputs to the IOP retrieval neural net is out of training range) was used for analysis (Brockmann *et al.* 2016).

2.2.3. POLYMER

The algorithm of POLYMER (POLYnomial based algorithm applied to MERIS) has been developed for MERIS data for removing influence of sun glint and retrieve ocean color parameters and ρ. POLYMER uses a spectral matching method using polynomial model, what models the spectral reflectance of atmosphere and sun glint. Furthermore, it is based on a ρ model and use all the bands in the visible part of the spectrum. Polynomial model contains of spectrally flat components (the residual sun glint, cloud reflectance, large particle scattering), aerosol signal and couplings between flat components and the Rayleigh scattering (Steinmetz *et al*. 2011). Bio-optical model uses chlorophyll and the backscattering coefficient of noncovarying particles (ESA 2012).

The AC processor of POLYMER is extended to other sensors such as S2/MSI. POLYMER (v1.1) is external tool that is used independently from SNAP. Output data contains chl-a, backscattering coefficient of non-covarying particles, ρ, quality flags, reflectance of the sun glint, wind speed predicted from ECMWF and TOA reflectance at 865 nm corrected for Rayleigh scattering (ESA 2012). Valid pixels were marked as 0 as water pixels with no flags.

2.2.4. Sen2Cor

Sen2Cor is developed for S2/MSI for generating and formatting Level 2 products. It performs AC for land applications and is capable for scene classification. Sen2cor classifies scenes into 12 classes (clouds, cloud shadows, vegetation, snow, water, cirrus etc). Sen2cor relies on a large database of look-up tables and atmospheric radiative transfer model. Level-2 products are generated at three resolutions: 10, 20 and 60 m. Resolution of 10 m contains bands 2, 3, 4 and 8, resolution of 20 m contains bands 2-7, 8a, 11 and 12 and resolution of 60 m contains all the bands.

Sentinel toolbox SNAP provides Sen2Cor (v2.1.2) processor for AC and scene classification. Output data of Sen2Cor are BOA reflectance images, aerosol optical thickness-, water vapour-, scene classification and quality indicators such as cloud and snow probability. For analyzing water quality, then only water pixels were used (Müller-Wilm *et al.* 2013).

2.3. Match-ups

For validating satellite data with *in situ* measurements S2/MSI Level-1 images were downloaded from Copernicus Open Access Hub (https://scihub.copernicus.eu/) from period 2015-2017. Match-ups were chosen by S2/MSI overpass and simultaneous *in situ* fieldworks on various waterbodies. *In situ* ρ from Tartu Observatory database were processed by S2/MSI Spectral Response Function (SRF) (v3.0) to compare ρ at the various bands. As weather in Estonia is challenging because of clouds then the range of the days between overpass and fieldwork was +/- 7 days and as sun angle is lower in autumn, then match-ups, where sun angle was lower than 30 degrees were not used. Downloaded images were processed by SNAP (v5) developed by Brockmann Consult, Array Systems Computing and C-S which is free open toolbox for processing data from Sentinel missions. As spatial resolution vary at different bands 60 m resampling was performed with Resampling (v2.0) tool. For identification of pixel types IdePix (v2.2) was used on Level-1 images for using only cloud-free pixels. Images were processed with previously mentioned AC processors such as C2RCC (v0.15), ACOLITE (v20170718.0), Sen2Cor (v2.1.2), POLYMER (v1.1). For analyzing match-up accuracy then 3x3 pixel area were used.

Used statistics will show differences between *in situ* data and S2/MSI data and help to decide accuracy of different AC processors. Following statistics were used for calculation: the coefficient of determination (R^2) (Equation 9), the average absolute percentage difference (ψ) (Equation 10), the root-mean-square difference (Δ) (Equation 11) and the bias (δ) (Equation 12). In the equations x_i is representing i-th *in situ* measurement, y_i is the i-th S2/MSI measurement and N is the number of match-ups (Qin *et al.* 2017).

$$R^2 = \frac{(\sum(x_i - \bar{x})(y_i - \bar{y}))^2}{\sum(x_i - \bar{x})^2 \sum(y_i - \bar{y})^2} \quad (9)$$

$$\psi = \frac{1}{N}\sum_{i=1}^{N}\left|\frac{y_i - x_i}{x_i}\right| * 100\% \quad (10)$$

$$\Delta = \sqrt{\frac{1}{N}\sum_{i=1}^{N}(y_i - x_i)^2} \quad (11)$$

$$\delta = \frac{1}{N}\sum_{i=1}^{N}\frac{y_i - x_i}{x_i} \quad (12)$$

2.4. Development of chl-a algorithms

For finding the best chl-a algorithms, *in situ* data collected during the FP7 GLaSS (Global Lakes Sentinel Services) was used. This dataset consists of simultaneous radiometric, IOP, chl-a, TSM data measured globally over eight optically different waterbodies and representing 412 data points.

Investigated algorithms are based on previously developed empirical algorithms, which are adjusted to S2/MSI wavelengths (Table 4). These 28 empirical algorithms are trained previously with different water types and are sensitive on different concentrations of OAS. In this study, algorithms were tested from oligotrophic to hyper eutrophic lakes and for estimating the best chl-a algorithms, coefficient of determination (Equation 9) was used.

Table 4. The form of the investigated algorithms, which were adjusted to S2/MSI wavelengths for this study.

Investigated empirical algorithms	**Reference**
R_{443}/R_{560}	Chavula *et al*. 2009
R_{490}/R_{443}	Salem *et al.* 2017
R_{490}/R_{560}	O'Reilly *et al*. 1998
$\log(R_{443}/R_{560})$	O'Reilly *et al*. 1998
$\log(R_{490}/R_{560})$	O'Reilly *et al*. 1998
$\ln(R_{490}/R_{560})$	Michell and Kahru 1998
$\ln(R_{443}/R_{560})$	Michell and Kahru 1998
$(R_{490}-R_{665})/(R_{560}-R_{665})$	Wozniak *et al.*2014
$(R_{490}-R_{443})/(R_{490}+R_{443})$	Salem *et al* 2017
$(1/R_{443}-1/R_{490})*R_{560}$	Salem *et al.*2017
$(R_{740}/R_{705})-(R_{740}/R_{665})$	Zimba and Gitelson 2006
R_{665}/R_{560}	Matthews *et al*. 2010
$1/R_{665}*R_{783}$	Moses *et al.* 2009
$1/R_{665}*R_{740}$	Moses *et al*. 2009
$1/R_{665}*R_{705}$	Moses *et al.* 2009
$1/R_{665}-1/R_{705}$	Gitelson *et al.*2009
$(1/R_{665}-1/R_{705})*R_{740}$	Gitelson *et al.* 2009, Gitelson *et al.* 2011 , Zhang *et al.* 2014
$(1/R_{665}-1/R_{705})*R_{783}$	Gitelson *et al.* 2009 , Gitelson *et al.* 2011 , Zhang *et al*. 2014
$(1/R_{665}-1/R_{705})/(1/R_{740}-1/R_{705})$	Zhang *et al*. 2014
$R_{705}-((R_{665}+R_{740})/2)$	Toming *et al*. 2016
R_{705}/R_{665}	Moses *et al.* 2009, Gitelson *et al.* 2009
$R_{740}*((1/R_{665})-1/R_{740}))$	Matthews *et al.*2010
$R_{705}/(R_{560}+R_{665})$	Matthews *et al.* 2010
$(1/R_{705}-1/R_{665})/(1/R_{705}+1/R_{665})$	Zhang *et al.* 2014
R_{740}/R_{665}	Gitelson *et al*. 2009
SPP	Zhang *et al.* 2017
MCI	Gower *et al*. 2008
FLH	Gower 1999

3. Results and discussion

3.1. Validation of water-leaving reflectance

Analyzing Tartu Observatory database, six match-ups from period 2015-2017 were found from May to September. Four previously described AC processors were used and match-ups are divided according to the S2/MSI overpass and fieldwork based on the 10 different waterbodies. Each ACs ρ were compared with Ramses TriOS ρ.

3.1.1. Match-up of Võrtsjärv

The first same day match-up is from 20th of May 2016 from Estonia second largest lake Võrtsjärv, which has the surface are of 270 km^2 and the average depth of the lake is 2.8 m (the deepest 6 m). Võrtsjärv belongs to Type 6 (non-stratified, water color light) according to the WFD (Table 1). The length of the Võrtsjärv is 34.8 km and the width is 14.4 km and is located in the middle of the Estonia. Lake Võrtsjärv is eutrophic lake with high chl-a and TSM (Table 5) and because of that the transparency is low. The color of the water is yellow-green or green-yellow and is caused by high amount of plankton and sediment from the bottom (Mäemets 1977, EELIS: Keskkonnaagentuur 2018). Point V1_1 is located in the middle of the lake and point V1_10 is near the shore at Limnology Station (Figure 4).

Table 5. Chl-a (mg/m^3), TSM (mg/l), a_{cdom} (m^{-1}) and Secchi depth (m) in Võrtsjärv

Point name	chl-a (mg/m^3)	TSM (mg/l)	a_{cdom} (442) (m^{-1})	Secchi depth (m)
V1_1	34.7	10.8	2.5	0.7
V2_10	34.8	10.8	2.4	0.7

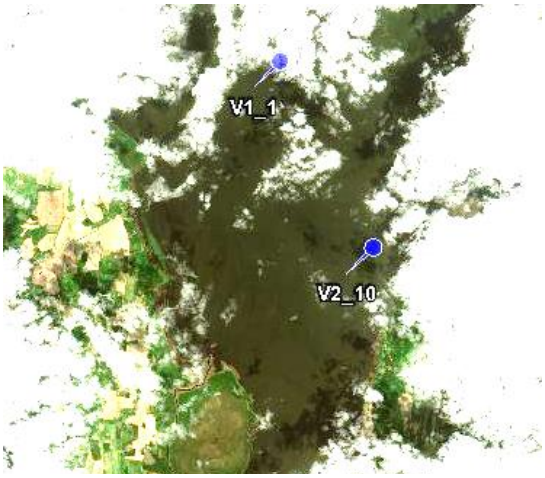

Figure 4. Locations of *in situ* measurements V1_1 and V2_10 locations in Võrtsjärv

As chl-a of Võrtsjärv is quite high (34-35 mg/m^3), all ρ spectrums show absorption peak near 675 nm (Figure 5a and b). ACs Polymer and C2RCC have similar shape of the ρ spectrum as *in situ* ρ spectrum. Polymer and C2RCC show little overestimation in the blue and red part of the ρ spectrum. ACOLITE and Sen2Cor overestimate ρ at all wavelengths, more pronounced in the blue part. The reason could be that ACOLITE and Sen2Cor are more sensitive to cloud pixels, which make the ρ higher, however cloud pixels were avoided. High TSM (10.8 mg/l) cause higher ρ at red/NIR wavelengths, which is shown by the results of all AC processors.

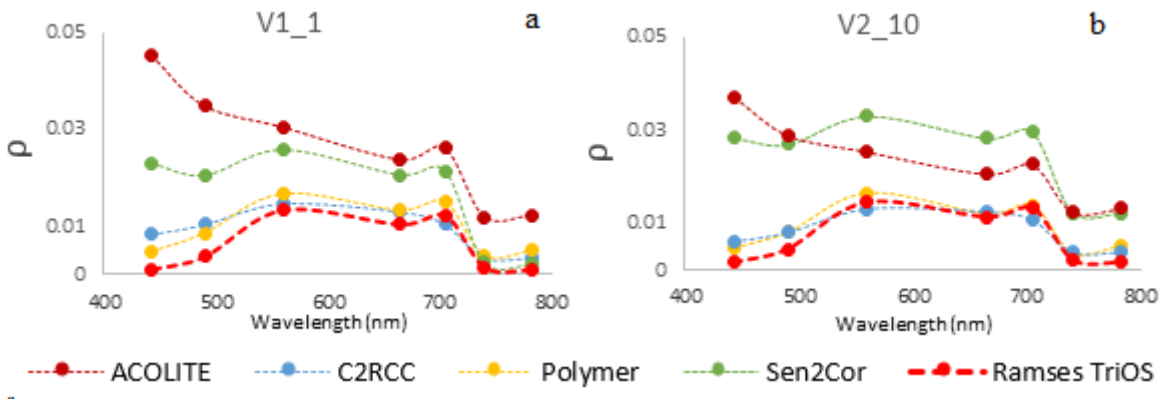

Figure 5. Water-leaving reflectance of Polymer, Sen2Cor, ACOLITE, C2RCC at point V1_1 (a) and point V2_10 (b) in Võrtsjärv

3.1.2. Match-up of Jõemõisa, Kaiu, Verevi, Pangodi

Match-up of small lakes from 28th of August 2016 is shown on the Figure 6 and the fieldwork was performed on 25th of August 2016. Both Jõemõisa and Kaiu are classified as Type 2 (non-stratified, color dark/light) waters according to the WFD (Table 1). The water surface of Jõemõisa (Figure 6a) is 71.6 hectares (ha) and it has an average depth of 2.6 m (the deepest 3.2 m). The length of Jõemõisa is 1.8 km and the width of the lake is 0.7 km. The surface of Kaiu (Figure 6b) is 134.4 ha and the average depth is 2.6 m (the deepest is 3 m). Kaiu is larger than Jõemõisa being 1.7 km long and 1.3 km wide. Jõemõisa and Kaiu lakes used to be one big lake centuries ago, but because of decreasing water level they have become separate lakes. Jõemõisa and Kaiu are located in the East side of Estonia. Lakes are eutrophic

with high chl-a (> 21 mg/m^3) and high. a_{cdom} (442) (> 10 m^{-1}), because both of them are located in the bog area (Table 6) and result in yellow-brown water color with a low transparency (0.8 m) (EELIS: Keskkonnaagentuur 2018, Mäemets 1977).

Verevi (Figure 6c) is small lake with 12.4 ha water surface area and an average of 3.6 m depth (the deepest 11 m). The length of the Verevi is 950 m and the width is 320 m. Verevi has been one of the permanent lake, where regular monitoring has been done. That is why it is included in WFD. Verevi is located in the middle of the Elva city in the South-East of Estonia. It is an eutrophic lake (chl-a 31 mg/m^3) with moderate transparency (1.4 m) (Table 6). Except East coast of Verevi, all the coast areas are swampy and the color of water is yellow (EELIS: Keskkonnaagentuur 2018, Mäemets 1977).

The fourth lake of this match-up is from Pangodi (Figure 6d). Pangodi has surface area of 93.3 ha and it is 2.1 km long and 720 m wide. It has an average depth of 3.9 m and the deepest depth is 11.1 m. The lake is located in the South-East side of Estonia and is located in between agricultural and forestry areas. Pangodi is eutrophic lake with moderate chl-a (15.2 mg/m^3) and relatively low TSM (4.2 mg/l) and a_{cdom} (442) (1.3 m^{-1}) (Table 6). The color of water is yellow-green or green-yellow with low to moderate transparency (1.7 m). Spring waters are very important sources for inflow water (EELIS: Keskkonnaagentuur 2018, Mäemets 1977). Verevi and Pangodi belong to Type 3 class based on the EU WFD (Table 1), where these lakes are representing stratified waters with dark/light water color.

Figure 6. Locations of in situ measurements in Jõemõisa (a), Kaiu (b), Verevi (c) and Pangodi (d) lakes

Table 6. Chl-a (mg/m^3), TSM (mg/l), a_{cdom} (m^{-1}) and Secchi depth (m) in Jõemõisa, Kaiu, Verevi and Pangodi

Lake	chl-a (mg/m^3)	TSM (mg/l)	a_{cdom} (442) (m^{-1})	Secchi depth (m)
Jõemõisa	27.3	4.3	10.1	0.8
Kaiu	21.2	5.0	14.0	0.8
Verevi	31.0	5.3	3.4	1.4
Pangodi	15.2	4.2	1.3	1.7

The results of ρ of match-up of 28th of August is represented on the Figure 7. As a_{cdom} (442) is high in Kaiu and Jõemõisa, the ρ spectrum is low at all wavelengths, because CDOM absorbs light really strongly. Only C2RCC gave results for these small lakes. The shape of C2RCC spectrums is similar to *in situ* ρ spectrum, but is overestimated in Jõemõisa (Figure 7a) and underestimated in Kaiu (Figure 7b). C2RCC is not showing chl-a absorption peak at 675 nm, but the chl-a is height in both lakes (> 21 mg/m^3).

As chl-a in Verevi (Figure 7c) is high as well (> 31 mg/m^3), then chl-a absorption peak at 675 nm is shown in *in situ* ρ spectrum. Only C2RCC gave results but the spectrum of ρ of C2RCC strongly underestimates the *in situ* ρ spectrum and does not show the chl-a absorption peak. Problems with the spectrum could be caused by the adjacency effect, which influences the pixels near coastline. Because Verevi is so small, ACs are not capable to distinguish water and vegetation line and water pixels are brighter than expected.

The *in situ* ρ spectrum of Pangodi (Figure 7d) is higher than previous lakes because of lower chl-a and a_{cdom} (442). Besides C2RCC, Sen2Cor gave results as well, probably because of the larger water surface area and the adjacency effect not having so high influence to water pixels. Both ACs underestimate *in situ* ρ spectrum, but the shape of both ρ spectrums are estimating *in situ* ρ spectrum well. Either C2RCC or Sen2Cor derived ρ does not show the chl-a absorption peak at 675 nm.

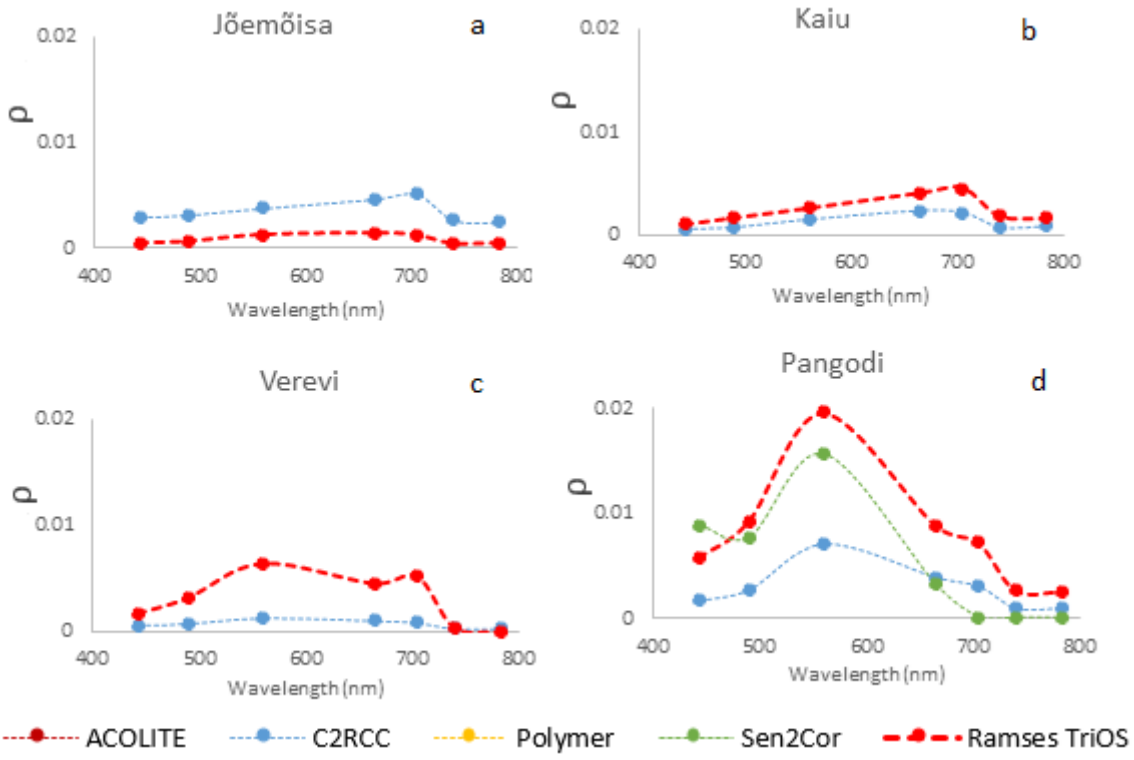

Figure 7. Water-leaving reflectance of Polymer, Sen2Cor, ACOLITE, C2RCC in Jõemõisa(a), Kaiu (b), Verevi (c) and Pangodi (d)

3.1.3. Match-up of Lake Peipsi

The third same day match-up is from Estonia biggest lake Peipsi (Figure 8) from 14th of September 2016. According to the WFD it is classified as Type 7 (non-stratified, water color light) (Table 1). The water surface area is 354 307 ha and the lake is divided into three parts: Peipsi (Northern part), Pihkva (Southern part) and Lämmijärv (connection between two parts). The length of the all Peipsi is 143 km and the width is 48 km. An average depth is 8 m and the maximum is 17.5 m in Lämmijärv. Peipsi is located in the Eastern part of Estonia and it is transboundary lake between Estonia and Russia. The concentrations of chl-a (24-35 mg/m^3) and TSM (10-16 mg/l) are high (Table 7) which is specific for eutrophic lake. The color of water is yellow-green or green-yellow and the transparency is moderate (0.6-0.9 m) in the open part of the lake (EELIS: Keskkonnaagentuur 2018, Mäemets 2977). *In situ* points are located in different parts of lake. Point Peipsi 11 is located in the middle of

the lake, but point Peipsi 12 and Peipsi 13 are located near the coastline. Point 38 in located in the mouth of river Suur-Emajõgi.

Table 7. Chl-a (mg/m^3), TSM (mg/l), a_{cdom} (m^{-1}) and Secchi depth (m) at Peipsi 11, Peipsi 12, Peipsi 13 and Peipsi 38 in Lake Peipsi

Point name	chl-a (mg/m^3)	TSM (mg/l)	a_{cdom} (442) (m^{-1})	Secchi depth (m)
Peipsi 11	25.5	10.5	1.6	0.9
Peipsi 12	34.3	12	4.8	0.7
Peipsi 13	35.4	15.7	5.8	0.6
Peipsi 38	24.8	12.5	1.9	0.8

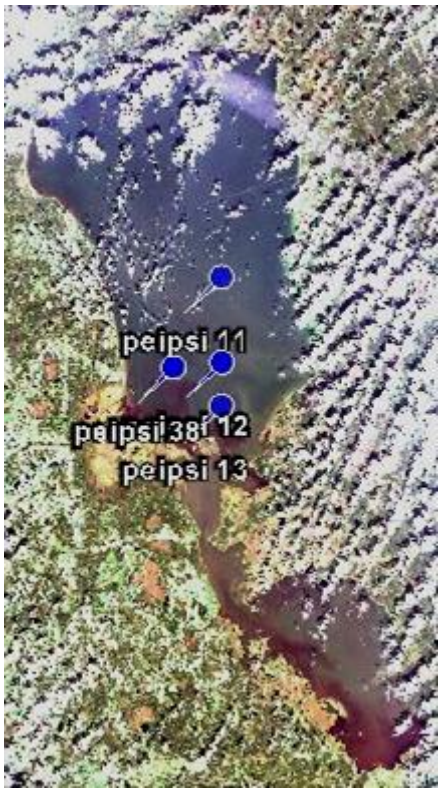

Figure 8. Locations of *in situ* measurements of Peipsi 11, Peipsi 12, Peipsi 13 and Peipsi 38 at Lake Peipsi

All AC processors are working well and ρ are comparable with *in situ* ρ spectrum (Figure 9). Point Peipsi 11 is located in the open part of the water, where chl-a and TSM are high and a_{cdom} (442) is low. On Figure 9a, the absorption peak of chl-a at 675 nm is shown and all the ACs are capable of estimating chl-a at this point. Polymer underestimates the most *in situ* ρ spectrum but otherwise the shape is similar. ACOLITE and Sen2Cor gave the same results of ρ as in Jõemõisa and Kaiu, where ρ are really high in the blue part of the spectrum. As a_{cdom} (442) is low then the values of ρ are higher.

Points Peipsi 12 (Figure 9b) and Peipsi 13 (Figure 9c) are located closer to the coastline of Peipsi. There is high chl-a, which is shown by chl-a absorption peak at 675 nm. Higher amount of a_{cdom} (442) (> 4.8 m^{-1}) results in lower ρ compared to Peipsi 11. Peipsi 13 is influenced by adjacency effect or bottom effect because it is located near the coast and in the shallow area of Peipsi. Because of these reasons, values of ρ are higher than *in situ* ρ, but the shape of the ρ spectrums are similar.

Peipsi 38 (Figure 9d) is located in river mouth and only C2RCC and Sen2Cor are working in these conditions. C2RCC is not showing good chl-a absorption peak at 675 nm as Sen2Cor (chl-a 24 mg/m^3). There is little overestimation of ρ by both ACs but the shapes of the ρ spectrums are estimated well.

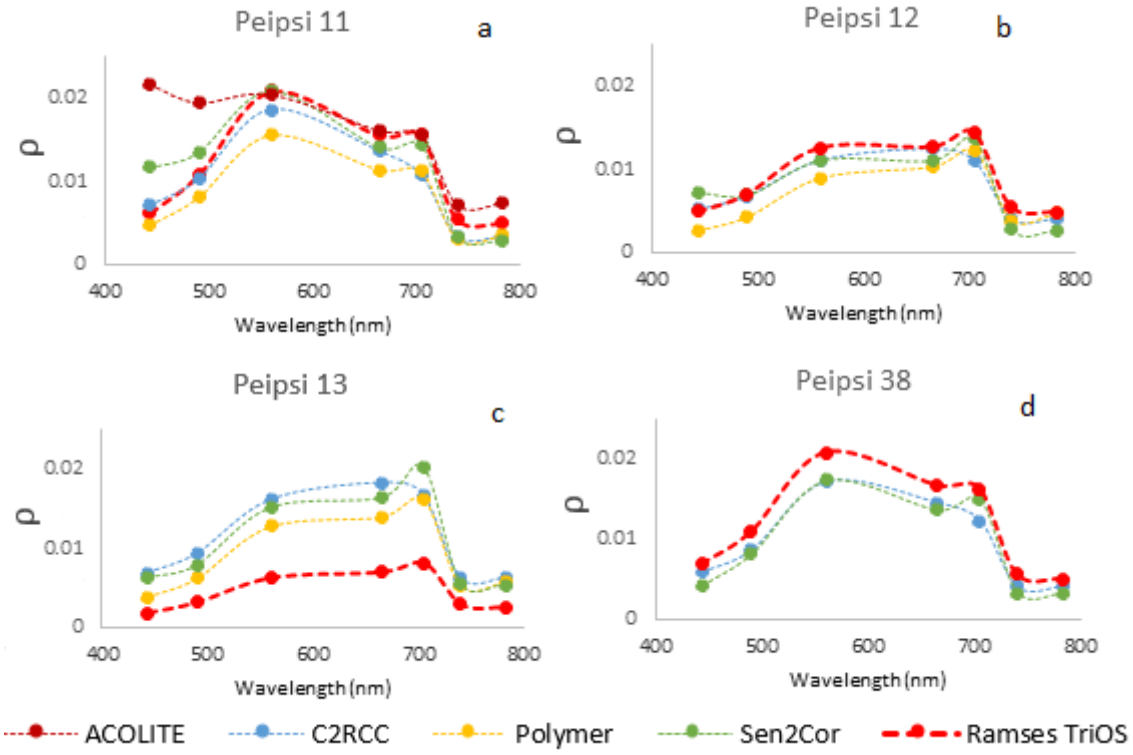

Figure 9. Water-leaving reflectance of Polymer, Sen2Cor, ACOLITE, C2RCC at points Peipsi 11(a), Peipsi 12(b), Peipsi 13(c) and Peipsi 38(d) in Lake Peipsi

3.1.4. Match-up of Pärnu Bay

Pärnu Bay is a part of Baltic Sea and is located in the South-West of Estonia next to Pärnu city. Between S2/MSI overpass and fieldwork there are 7 days, fieldwork was done 7th of July 2018 and S2/MSI image from 14th of July. The salinity of Pärnu Bay depends on the season: in spring it could be even 0 ‰ and in winter up to 6‰. As River Pärnu flows into Pärnu Bay and the amount of inflow of river water is high, the salinity is not as high as in Baltic Sea. Pärnu bay is eutrophic, because of inflow from Pärnu River that influences the

quality of water. The river brings suspended matter from river shores, therefore concentrations of OAS are high. (TÜ Eesti Mereinsituut 2013).

The *in situ* points of Pärnu Bay are located from coast to open Baltic Sea (Figure 10). Chl-a TSM and a_{cdom} (442) decrease from coast along Baltic Sea. As point Pärnu 1 is located in the river mouth then chl-a (27 mg/m^3) and TSM (9.2 mg/l) are high (Table 8). At Pärnu 7, which is located in open sea, chl-a (7.3mg/m^3) and TSM (4.3 mg/l) are lower. Secchi depth increase, because of lower concentrations of OAS.

Table 8. Chl-a (mg/m^3), TSM (mg/l), a_{cdom} (m^{-1}) and Secchi depth (m) at Pärnu 1, Pärnu 2, Pärnu 3, Pärnu 6 and Pärnu 7 in Pärnu Bay

Point name	chl-a (mg/m^3)	TSM (mg/l)	a_{cdom} (442) (m^{-1})	Secchi depth (m)
Pärnu 1	27.0	9.2	3.3	0.9
Pärnu 2	6.3	6.7	1.2	1
Pärnu 3	5.7	8.5	1.0	1.1
Pärnu 6	8.3	7.3	0.9	1.2
Pärnu 7	7.3	4.3	0.8	1.5

Figure 10. Locations of *in situ* measurements of Pärnu 1, Pärnu 2, Pärnu 3, Pärnu 6 and Pärnu 7 in Pärnu Bay

As chl-a is high at the point Pärnu 1 then on the first graph (Figure 11b) spectrum of *in situ* ρ illustrates chl-absorption peak near 675 nm. ACs do not show very good chl-a absorption and overestimate the *in situ* ρ spectrum. The best results shows Polymer, which shows best agreement with *in situ* ρ spectrum in terms of the values and the shape of the spectrum As Pärnu 1 is in shallow water, the overestimation could be caused by the combination of adjacency effect and bottom effect.

All the ACs are working well at point Pärnu 2 (Figure 11b) because the shape of the ρ spectrum and ρ are similar with *in situ* ρ spectrum. As previously seen, in Võrtsjärv and Peipsi, ACOLITE overestimates the blue part of the spectrum.

The ρ in station Pärnu 3 (Figure 11 c) is overestimated by all AC processors, which could be due to the adjacency effect as the point is located in the narrower area of the bay and is influenced by the coast. Polymer and C2RCC estimates *in situ* ρ spectrum well and Sen2Cor overestimates the most of it. Point Pärnu 3 is close to the clouds as well, which could influence the spectrum of ρ, although all the used pixels are classified as 'water pixels'.

Points Pärnu 6 and Pärnu 7 (Figure 11 e and f) are measured further away from the coast and therefore are showing better results than previous points. As Pärnu 7 is located in the open sea and chl-a, TSM and a_{cdom} (442) are low, then the ρ are lower as well. ACOLITE continuously overestimates the blue part, but other ρ of ACs give similar results than *is situ* ρ spectrum.

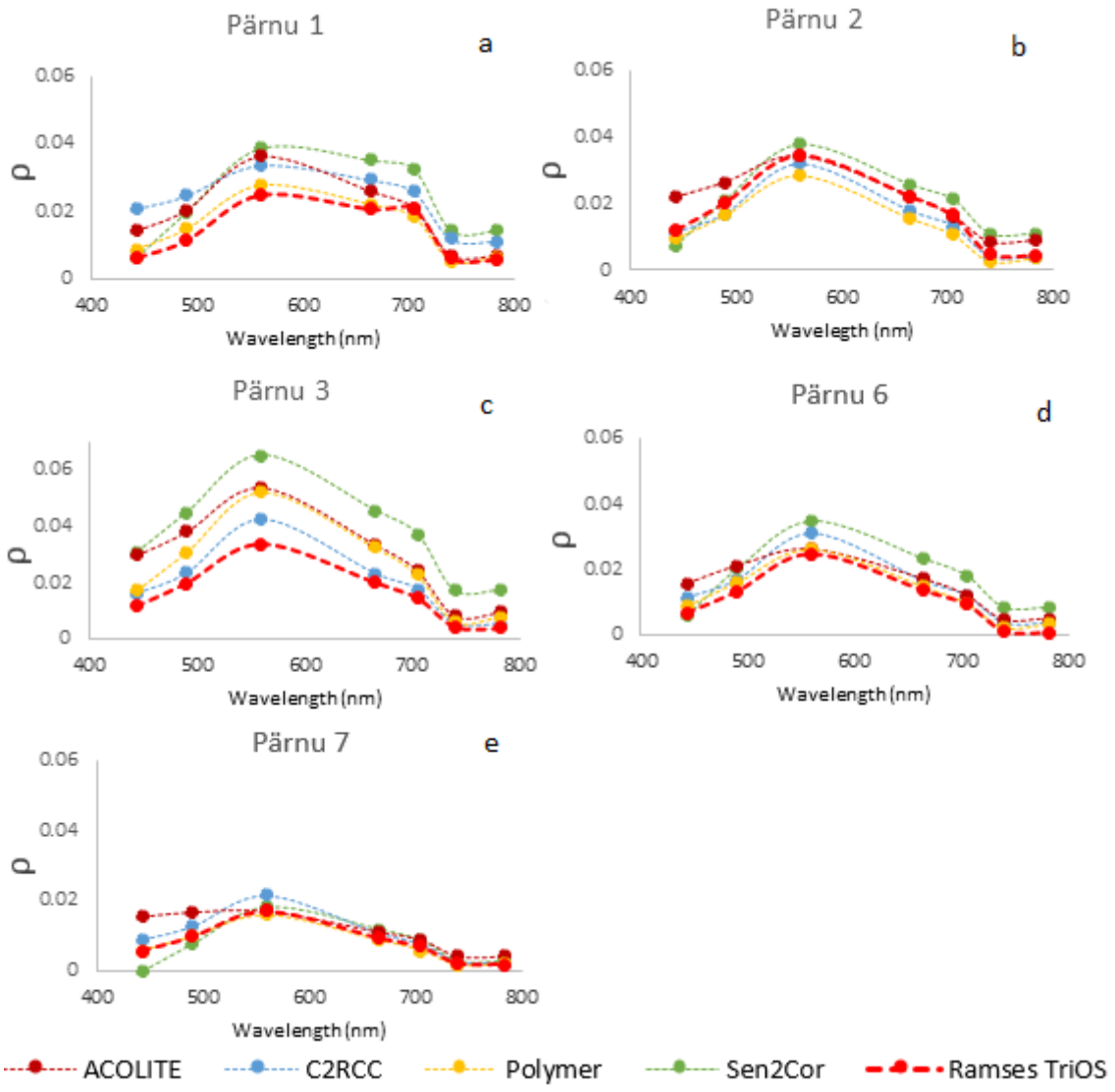

Figure 11. Water-leaving reflectance of Polymer, Sen2Cor, ACOLITE, C2RCC at points Pärnu 1 (a), Pärnu 2 (b), Pärnu 3 (c), Pärnu 6 (d) and Pärnu 7 (e) in Pärnu Bay

3.1.5. Match-up of Otepää Valgjärv

Otepää Valgjärv (Figure 12) is small lake with 65.8 ha surface area and is located in the South-East of Estonia. The same day match-up is from 28th of August 2017 and Otepää Valgjärv is classified as Type 2 (non-stratified, color dark/light) based on the EU WFD (Table 1). The lake is 1.4 km long and 0.8 km wide, with an average depth of 3.2 m and with, maximum depth of 5.5 m. It is surrounded with a forest areas on one side and agricultural areas on the other. The lake is eutrophic lake, where chl-a is above 25 mg/m^3 and TSM is also over 25 mg/l (Table 9). The water of the lake is green-yellow with a low transparency (1.3 m) (EELIS: Keskkonnaagentuur 2018, Mäemets 1977).

Table 9. Chl-a (mg/m^3), TSM (mg/l), a_{cdom} (m^{-1}) and Secchi depth (m) in Otepää Valgjärv

Lake	chl-a (mg/m^3)	TSM (mg/l)	a_{cdom} (442) (m^{-1})	Sechhi depth (m)
Otepää Valgjärv	27.1	25.5	1.7	1.3

Figure 12. Location of *in situ* measurement of Otepää Valgjärv

As the chl-a is high in Otepää Valgjärv, strong chl-a absorption peak is showed at the 675 nm (Figure 13) by *in situ* ρ, but is not detected by any of AC processors. The ρ of ACs are different than *in situ* ρ spectrum and rather underestimate the *in situ* ρ spectrum. Similar ρ spectrum to *in situ* ρ spectrum has Sen2Cor with a slight absorption peak at 675 nm, but underestimation in the blue part of the ρ spectrum and above 750 nm. ACOLITE does not work and Polymer and C2RCC are showing rather clean water spectrum than eutrophic water spectrum with high chl-a in water. As Otepää Valgjärv is small lake then adjacency effect affects the results of ρ of ACs. Pixels could be affected by the vegetation pixels and ACs are not able to identify water pixels even if they classify these as water pixels.

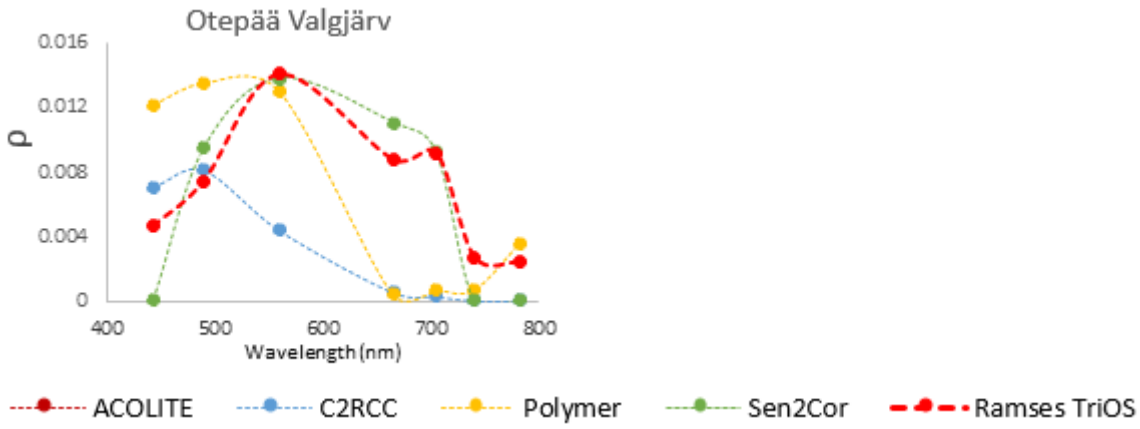

Figure 13. Water-leaving reflectance of Polymer, Sen2Cor, ACOLITE, C2RCC in Otepää Võrtsjärv

3.1.6. Match-ups of Kirikumäe, Murati and Hino

The same day match-ups of Kirikumäe, Murati and Hino lakes are from 30 of August 2017 (Figure 14). Lakes are located in the southern part of Estonia and are classified as Type 5 (non-stratified, water color light), Type 3 (stratified, water color dark/light) and Type 2 (non-stratified, water color dark/light) (Table 1) respectively. The water surface area of Kirikumäe (Figure 14a) is 62 ha and has an average depth of 2.8 m (deepest 3.5 m). The lake is 1 km long and 950 m wide and is surrounded by low and swampy areas. Kirikumäe is rare non-stratified eutrophic semi-humus lake, where concentrations of OAS are high (Table 9), because most of the water is coming from the swampy areas. The color of water is yellow to brown-yellow with a low to moderate transparency (EELIS: Keskkonnaagentuur 2018, Mäemets 2018).

Murati (Figure 14b) has surface are of 66 ha, with an average depth of 3.6 m (maximum depth is 4.3 m). The lake is narrow in the middle and the length of the lake is 1.8 km whereas the width is 700 m. It is surrounded by agricultural clay soil and sand soil forestry areas. Murati is eutrophic lake where the chl-a is over 20 mg/m^3 and a_{cdom} (442) over 10 m^{-1} (Table 10). The color of water is yellow with low transparency because of CDOM (EELIS: Keskkonnaagentuur, Mäemets 1977)

Hino (Figure 14c) is located between forest areas and the water surface is 207 ha and it is 2.9 km long and 1.2 km wide. The average depth is 3.1 m whereas the maximum depth is

10.4 m. TSM is high (10.7 mg/l), but the water is described as transparent and light to yellow-green (EELIS: Keskkonnaagentuur 2018, Mäemets 1977).

Figure 14. Locations of *in situ* measurements of Kirikumäe (a), Murati (b) and Hino (c) lakes

Table 10. Chl-a (mg/m^3), TSM (mg/l), a_{cdom} (m^{-1}) and Secchi depth (m) in Kirikumäe, Murati and Hino lake

Lake	chl-a (mg/m^3)	TSM (mg/l)	a_{cdom} (442) (m^{-1})	Secchi depth (m)
Kirikumäe	20.7	6.0	7.7	1.2
Murati	23.8	3.7	13.3	1
Hino	5.3	10.7	0.7	-

As a_{cdom} (442) is high in Kirikumäe (Figure 15a) and Murati (Figure 15 b), then *in situ* ρ is low and specific for CDOM dominated waters. C2RCC and Sen2Cor give results in those cases, but these are overestimating in the blue part of the ρ spectrum and underestimating in the red part of the ρ spectrum.

Hino is larger and deeper lake than previous lakes and the amount of OAS are lower (Figure 15c). Water-leaving reflecntances are high because of high TSM. The shape of the ρ spectrum is the best with C2RCC, but it strongly underestimates *in situ* ρ spectrum, Polymer is estimating the values of ρ similar at 560 nm as *in situ* ρ, but overestimates in the blue part and underestimates in the red part of the ρ spectrum. Sen2Cor is similar as C2RCC, but the values of ρ in the blue part are higher. As specific to ACOLITE is in small lakes, it flagged out all the pixels.

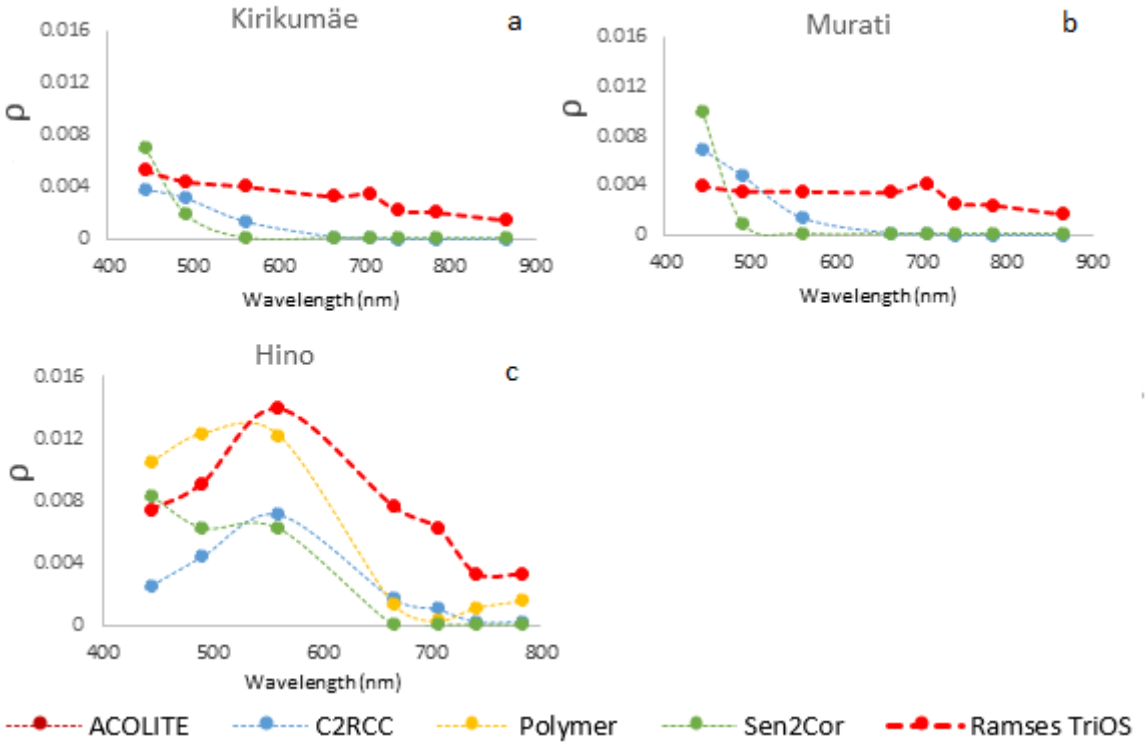

Figure 15. Water-leaving reflectance of Polymer, Sen2Cor, ACOLITE, C2RCC in Kirikumäe, Murati and Hino

3.1.7. Comparison of atmospheric corrections

For comparing ACs in different levels of OAS in water with *in situ* measurements, it was noticed that adjacency effect could cause problems with estimating correct ρ spectrum in small lakes. However, C2RCC is capable to derive ρ in most cases and especially in CDOM dominated waters. C2RCC is working in every water type and Sen2Cor in same CDOM dominated waters, although fails more often than C2RCC. ACOLITE does not work in small lakes and typically overestimates, similarly to Sen2Cor's, strongly the blue part of the ρ spectrum in big lakes and coastal areas. Polymer is working well in TSM dominated small lakes

Each AC was analyzed by given statistics based on the statistics derived by Equation 9, 10, 11, 12 and compared with *in situ* ρ. For finding the best AC processor for this study all the characteristics were considered. Results of comparison of four ACs are represented on the Table 11.

Table 11. Comparison of AC processors (ACOLITE, C2RCC, Sen2Cor, Polymer) at S2/MSI wavelengths based on the calculated statistics

ACOLITE N=8	443	490	560	665	705	740	783
R^2	0.23	0.01	0.46	0.37	0.23	0.01	0.01
ψ	910.96	224.25	39.71	44.19	39.49	228.93	356.82
Δ	0.02	0.02	0.01	0.01	0.01	0.01	0.01
δ	9.11	2.24	0.39	0.44	0.39	2.29	3.57
slope	-1.36	0.10	0.95	0.83	0.68	-0.15	-0.21
intercept	0.03	0.02	0.01	0.01	0.01	0.01	0.01
C2RCC N=19							
R^2	0.27	0.57	0.78	0.72	0.70	0.33	0.28
ψ	113.68	57.62	43.70	49.30	50.73	74.65	115.40
Δ	0.00	0.00	0.01	0.00	0.00	0.00	0.00
δ	0.74	0.15	-0.14	-0.19	-0.31	-0.03	0.47
slope	0.86	0.99	1.15	1.23	1.19	0.99	0.95
intercept	0.00	0.00	0.00	0.00	0.00	0.00	0.00
Polymer N=13							
R^2	0.43	0.59	0.67	0.49	0.37	0.12	0.05
ψ	85.48	49.66	26.58	38.53	38.87	62.97	106.51
Δ	0.00	0.00	0.01	0.01	0.01	0.00	0.00
δ	0.66	0.31	0.06	-0.06	-0.10	0.10	0.89
slope	0.80	0.97	1.13	1.12	0.90	0.33	0.23
intercept	0.00	0.00	0.00	0.00	0.00	0.00	0.00
Sen2Cor N=16							
R^2	0.00	0.35	0.69	0.61	0.57	0.09	0.06
ψ	297.13	100.68	52.95	65.78	64.16	147.64	188.97
Δ	0.01	0.01	0.01	0.01	0.01	0.01	0.01
δ	2.61	0.74	0.18	0.24	0.25	0.84	1.26
slope	-0.10	1.26	1.52	1.77	1.79	1.03	0.96
intercept	0.01	0.00	0.00	0.00	0.00	0.00	0.00

Number of pixels for comparison within ACs was highest for C2RCC (N = 19), which gives opportunity to get information from small lakes. The least water pixels was given by ACOLITE, because it flagged out all the water pixels of small lakes, which makes this algorithm difficult to apply for small lakes. Coefficient of determination shows the highest correlation in all ACs at the wavelengths 560, 665 and 705 nm, which are the main wavelengths for developing chl-a algorithms for Case 2 waters. C2RCC shows the highest correlation ($R^2 > 0.7$) at these wavelengths, whereas in other ACs, the correlation is smaller ($R^2 < 0.7$). Intercept is zero in C2RCC, Polymer and Sen2Cor, what indicates that these ACs

ρ fit well with the *in situ* ρ. ACOLITE gives higher intercept values (intercept > 0.1). Slope near to one indicates, that AC ρ and *in situ* ρ, fit well with each other. At main wavelengths of developing chl-a algorithms, the slope was closer to ones in C2RCC (slope = 1.15-1.23) and Polymer (slope = 0.90-1.12).

Based on the average absolute percentage difference values, Polymer gives the most accurate results compared to the *in situ* ρ results at the main chl-a developing wavelengths ($\psi < 39.0$). Even ACOLITE is comparable with Polymer, because it gives smaller average absolute percentage difference values than C2RCC. According to the root-mean-square difference, C2RCC shows the most accurate results and shows that C2RCC is the most comparable with *in situ* ρ, only at 560 nm $\Delta = 0.01$, otherwise it was 0. As bias indicates over- or underestimation C2RCC rather underestimates the *in situ* ρ spectrum than other ACs.

Based on the derived statistics, C2RCC and Polymer come forward. As the purpose of the study is to estimate water quality in small lakes, the high number of water pixels is essential value, which is highest in case of C2RCC. Based on the coefficient of determination and root-mean-square difference (whereas for C2RCC Δ value is zero at every wavelength (except 560 nm), but Polymer shows $\Delta = 0.01$ at three wavelengths.), the C2RCC was selected as a processor to derive the ρ as input for chl-a algorithms.

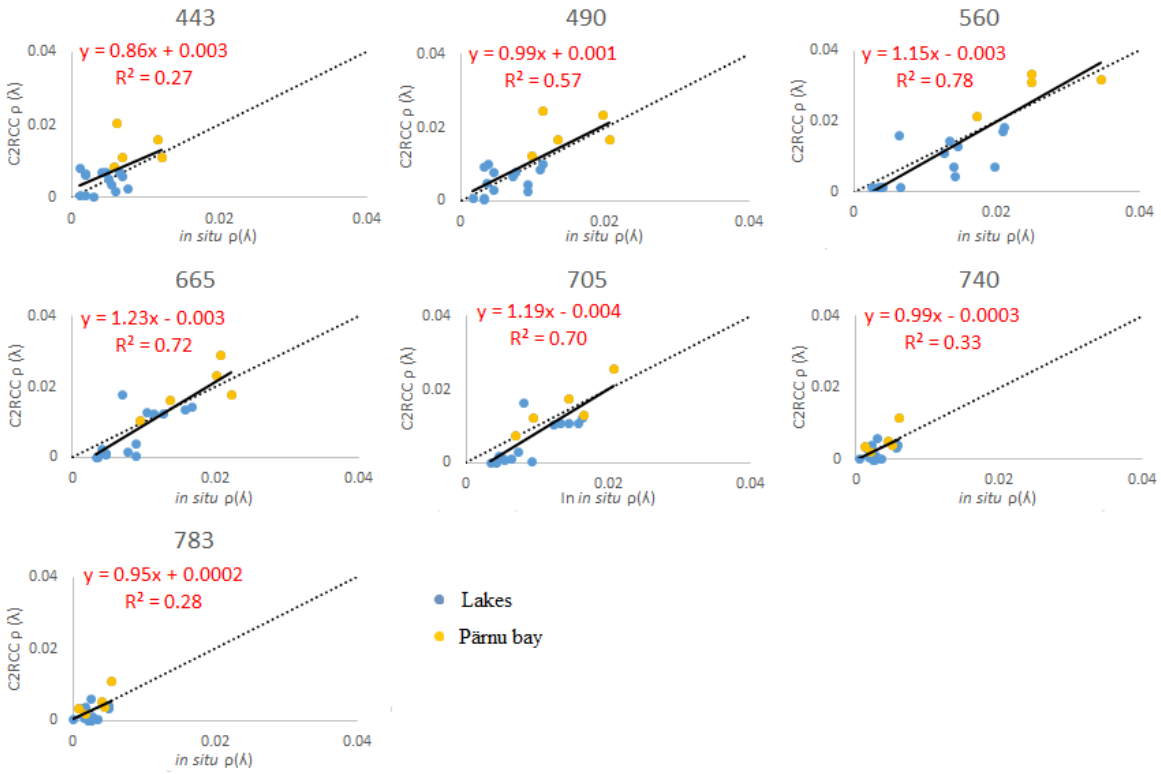

Figure 16. Comparison of C2RCC ρ(λ) versus *in situ* ρ(λ) at S2/MSI wavelengths. Dotted line represent 1:1 line and dark constant line is the trendline.

As C2RCC was chosen for AC procedure, it is important to know the specific correlation at given wavelengths. Figure 16 shows correlation between C2RCC ρ and *in situ* ρ at given wavelengths, where yellow points represent Pärnu Bay points and blue points lakes. Lake values of C2RCC ρ are rather underestimated compared with *in situ* ρ values. Table 11 supports the underestimation because the bias is negative from 560 nm. Pärnu Bay points are showing better accuracy and are located more near to the 1:1 line.

3.2. Comparing and developing chl-a algorithms for S2/MSI

Second part of the study was to analyze chl-a algorithms applicable for S2/MSI data. First, as MSI sensor has wide bands (Figure 2) around chl-a absorption peak, the sensitivity analyses was performed based on the *in situ* measured ρ, which was processed in parallel with MSI and OLCI's Spectral Response Function (SRF). The chl-a retrievals by Three-

Band NIR-Red Model and Four-Band NIR-Red Model algorithms applied on TriOS RAMSES (Figure 17a,b) and simulated S2/MSI (Figure 17c,d) and OLCI (Figure 17e,f). The data show the potential of S2/MSI to derive chl-a over wide range of values with comparable accuracy (S2/MSI R^2 = 0.52 and 0.68) to OLCI (S3/OLCI R^2 = 0.50 and 0.66) results independently from different algorithm. Based on these results, the location and width of the S2/MSI spectral bands are suitable to derive chl-a, but low SNR could cause bigger uncertainties.

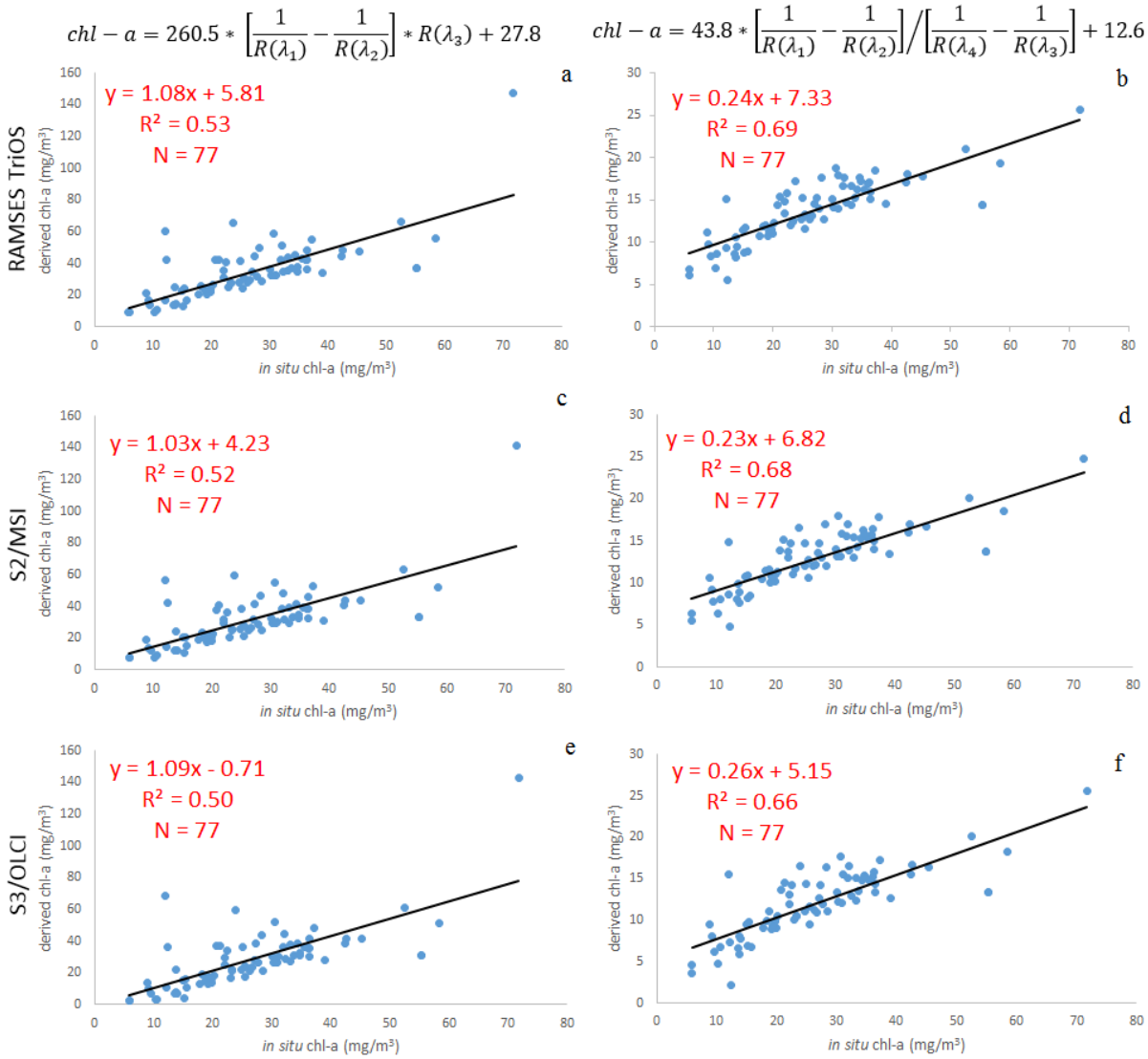

Figure 17. Comparison of derived chl-a (mg/m^3) of Ramses TriOS, S2/MSI and S3/OLCI and *in situ* chl-a (mg/m^3) based on the Three-Band NIR Red Model and Four-Band NIR Red Model algorithms.

To analyze the performance of various empirical approaches, all algorithms (Table 4) were applied on the GLaSS dataset, where different water types were represented. For every water type (or lake), three best empirical approaches were chosen based on the R^2 values between *in situ* and S2/MSI data (Table 12).

The highest correlation between tested empirical approaches and corresponding chl-a were retrieved in Võrtsjärv and Vesijärv, which gave $R^2 > 0.92$ and $R^2 > 0.94$, respectively. Two-Band NIR-Red Model algorithms are working better in the low CDOM waters (a_{cdom} (442) < 4.1 m^{-1}). The best band ratio model is based on R_{705}/R_{665} for eutrophic (e.g Taihu (R^2 = 0.46), Vesijärv (R^2 = 0.97)) to oligotrophic (e.g. Garda (R^2 = 0.2)) waters. As Three-Band NIR-Red Model based algorithms are working for turbid waters, good correlation for simpler band ratio algorithm $(1/R_{665}-1/R_{705})*R_{740}$ for Peipsi (R^2 = 0.40) and Võrtsjärv (R^2 = 0.92) and $(1/R_{665}-1/R_{705})*R_{783}$ for Võrtsjärv (R^2 = 0.93) and for Peipsi (R^2 = 0.38), was used. Four-Band NIR-Red Model algorithms are showing good results in TSM dominated waters like Peipsi (R^2 = 0.4) Võrtsjärv (R^2 = 0.92) and Taihu (R^2 = 0.46). In Maggiore, where concentration of OAS are low, the blue and green bands ratio algorithms work better, for example R_{490}/R_{443} (R^2 = 0.31). MCI algorithm (index 0.339) is showing good correlation in Finnish boreal lakes (R^2= 0.83) and Betuwe area (R^2 = 0.87), which has relatively different water types based on the chl-a (Betuwe chl-a median = 23.5 mg/m^3 and Finnish boreal lakes chl-a median = 3.2 mg/m^3) and TSM (Betuwe TSM max = 28.2 mg/l and Finnish boreal lakes TSM max = 2.1 mg/l).

Table 12. Based on the GLaSS dataset, three algorithms for every waterbody were selected based on the R^2. As every lake concentrations of OAS are different then minimum, maximum and average concentrations are shown on the table. Equation for deriving chl-a is shown on the last row.

	chl-a (mg/m^3)	TSM (mg/l)	a_{cdom} (442) (m^{-1})	Secchi depth (m)	algorithms			
					N	R^2	band ratios	equation
Peipsi	2.7 -14.3 (7.5)	1.9-11.7 (6.3)	1.7-4.1 (2.3)	0.8 -2.65 (1.4)	23	0.44	$1/R_{665}$-$1/R_{705}$	y = 0.1x + 9.8
						0.40	$(1/R_{665}$-$1/R_{705})*R_{740}$	y = 65.0x + 10.2
						0.40	$(1/R_{665}$-$1/R_{705})/(1/R_{740}$-$1/R_{705})$	y = 43.2x + 10.2
Võrtsjärv	24.6-45.3 (35.8)	10.0-18.7 (15.7)	2.2-4.2 (2.6)	0.45 -0.7 (0.6)	11	0.93	$(1/R_{665}$-$1/R_{705})*R_{783}$	y = 286.1x + 27.7
						0.92	$(1/R_{705}$-$1/R_{665})/(1/R_{705}$+$1/R_{665})$	y = -165.0x + 27.9
						0.92	$(1/R_{665}$-$1/R_{705})*R_{740}$	y = 260.5x + 27.8
Betuwe	12.1-150.2 (23.5)	1.4-28.2 (4.6)	N/A (N/A)	N/A (N/A)	16	0.83	$(R_{665}$-$R_{705})$-$0.339*(R_{783}$-$R_{665})$	y = 27639.6x + 13.7
						0.82	$(R_{665}$-$R_{705})$-$0.389*(R_{783}$-$R_{665})$	y = 26772.0x + 11.5
						0.77	R_{705}-$((R_{665}$+$R_{740})/2)$	y = 24385.4x + 7.7
Finnish boreal lakes	1.6-8.2 (3.2)	0.7-2.1 (1.9)	0.8-10.3 (1.4)	1.3 -5 (3.5)	9	0.87	$(R_{665}$-$R_{705})$-$0.339*(R_{783}$-$R_{665})$	y = 20821.5x + 1.7
						0.83	$R_{705}/(R_{560}/R_{665})$	y = 4313.1x + 0.6
						0.82	$(R_{665}$-$R_{705})$-$0.389*(R_{783}$-$R_{665})$	y = 16649.4x + 1.5
Vesijärv	1.7-11.0 (4.6)	1.2-3.4 (2.5)	0.5-0.9 (0.8)	2.4 -4.6 (2.9)	7	0.97	R_{705}/R_{665}	y = 29.4x -15.8
						0.95	$(1/R_{705}$-$1/R_{665})/(1/R_{705}$+$1/R_{665})$	y = -43.8x - 12.6
						0.94	$(R_{490}$-$R_{665})/(R_{560}$-$R_{665})$	y = -23.8x + 11.1
Garda	0.2-9.2 (1.3)	0.2-14.7 (1.4)	0.0-1.2 (0.1)	0.8 -8.5 (4.5)	46	0.25	$(R_{490}$-$R_{665})/(R_{560}$-$R_{665})$	y = -2.7x + 3.9
						0.21	$(1/R_{705}$-$1/R_{665})/(1/R_{705}$+$1/R_{665})$	y = -4.1x + 2.5
						0.20	R_{705}/R_{665}	y = 2.2x + 0.1
Maggiore	0.2-3.8 (1.6)	0.1-2.8 (0.6)	0.1-0.6 (0.2)	4.9 -10.5 (8.5)	57	0.31	R_{490}/R_{443}	y = 6.5x - 7.7
						0.30	$\ln(R_{443}/R_{490})$	y = -9.3x - 1.7
						0.30	$(R_{490}$-$R_{443})/(R_{490}$+$R_{443})$	y = 19.1x - 1.8
Taihu	4.0-942.6 (16.9)	11.2-285.6 (54.3)	0.2-2.3 (0.8)	0 -0.9 (0.3)	243	0.46	R_{705}/R_{665}	y = 125.9x - 101.5
						0.46	$(1/R_{705}$-$1/R_{665})/(1/R_{705}$+$1/R_{665})$	y = -461.9x - 25.8
						0.45	$\ln(R_{490}/R_{560})$	y = -359.9x - 110.8

3.3. Deriving ecological status of water based on chl-a

During the derivation of the ecological status of water based on the chl-a algorithms, dynamics of chl-a often remains constant and does not have the seasonal dynamics as present in *in situ* data. Spectrums of ρ were further investigated.

For example in case of eutrophic lake Verevi (Figure 18), with surface area of 12.4 ha, some of the water pixels are not typical Case 2 pixels (Figure 18b), because shorter wavelengths

have higher ρ values than longer wavelengths and the values at 665 nm and adjacent bands are very low and similar. This in turn results in constant chl-a concentration.

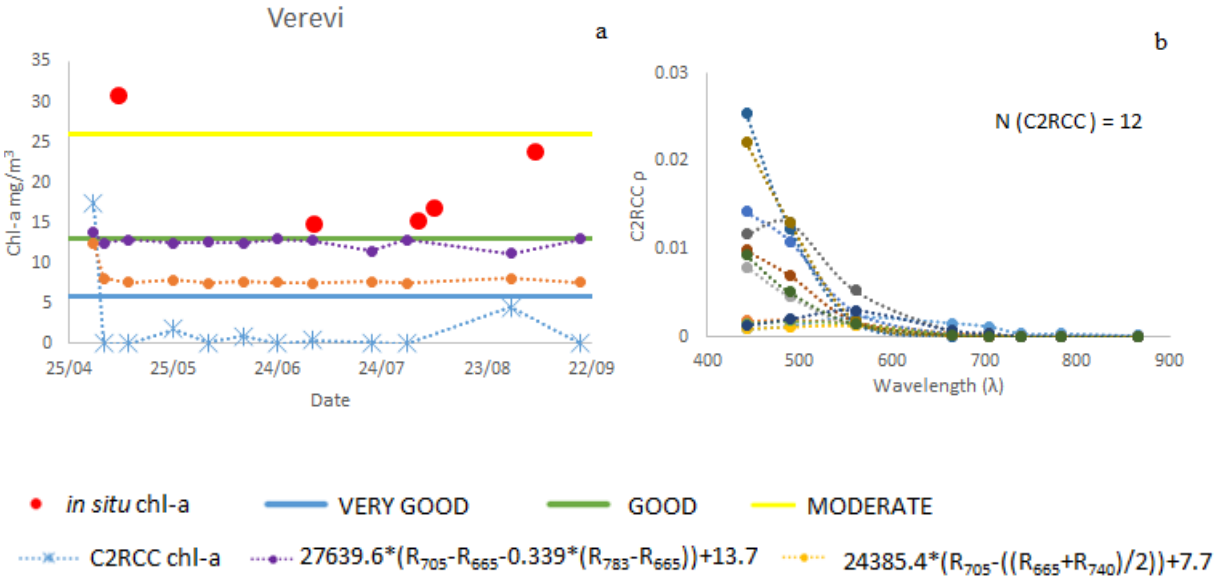

Figure 18. Estimation of chl-a seasonal dynamics in Verevi in 2017 (a) and C2RCC derived ρ (b),

3.3.1. Spatial analyses on C2RCC derived ρ product

Applying C2RCC on various S2/MSI data, it revealed that in case of smaller lakes, especially with sophisticated shoreline, the AC often failed and derived the invalid ρ – highest value at first band and constantly decreasing towards longer wavelengths.

As ρ spectrums were not the typical Case 2 spectrums, then further investigation was done. As previously investigated wide band 665 nm should not be a problem for not deriving accurate chl-a, therefore C2RCC were investigated by visual analyzation. In optically complex waters as Estonian small lakes are, pixels should have smaller values of ρ in the blue part of the ρ spectrum than in red part of the ρ spectrum. For analyzing water pixels in small lakes, condition band 3 (band at 560 of C2RCC) < band 1 (band at 443 of C2RCC) were applied to C2RCC image to find out invalid pixels or cases when the equation was true. For analyzing pixels, one narrow lake Raigastvere and bigger lake Saadjärv were investigated in 2016.

The first image was processed by IdePix, which classifies pixels (water pixels are showed in black) (Figure 19). Another images are C2RCC images, where water pixels are shown in black color as well, whereas red pixels are representing pixels were condition band 3 < band 1 is true. In other words, 'Red pixels' are not true Case 2 pixels. Raigastvere water surface is 11 hectares and the lake is narrow (510 m). In all images, pixels what are located near the coastal area are marked as not true Case 2 pixels. It is caused by adjacency effect, where vegetation is influencing water pixels. C2RCC is not able to process pixels near shore, because these pixels are mixed. All the pixels are invalid in the end of the June (29/06/2016) which is most likely caused by algae in the water surface.

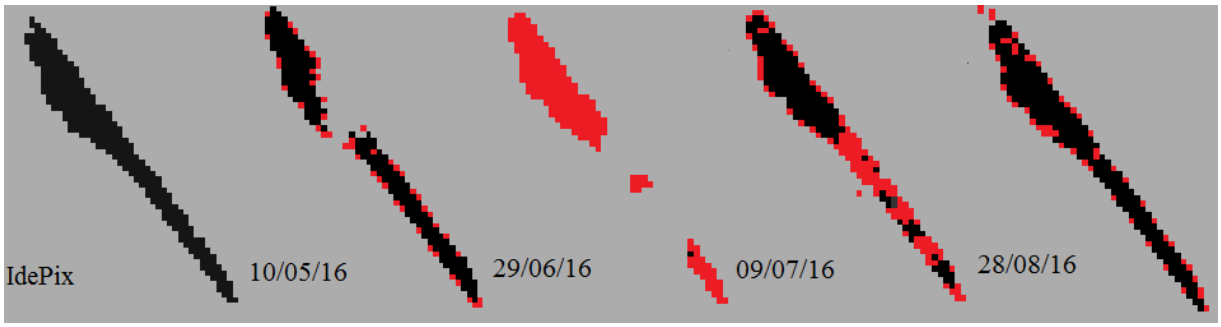

Figure 19. Time series of Raigastvere, where 'Red pixels' are showing the condition band 3 < band 1 and 'Black pixels' are representing water pixels.

Figure 20 shows the difference between 'Red pixels' and 'Black pixels' (randomly selected from Raigastvere). Spectrum of 'Black pixels' is typical ρ spectrum, where ρ is low in the shorter wavelengths and increases at longer wavelengths until 700 nm. Therefore 'Red pixels' spectrum is rather clear water spectrum than typical Case 2 spectrum, where ρ of the blue part is high.

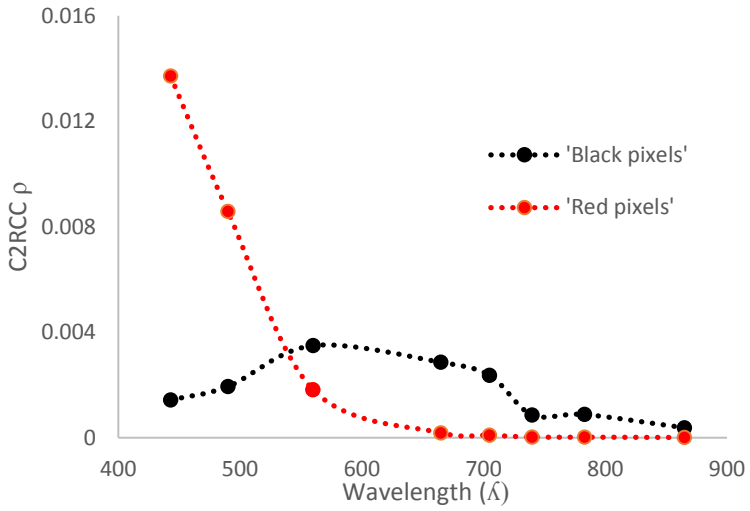

Figure 20. Spectrums of 'Black pixels' and 'Red pixels'

As Raigastvere is a narrow lake, Saadjärv was investigated as well, as a larger and wider lake. Saadjärv is 1.8 km wide and has an average depth of 8 meters. It means that adjacency and bottom effect should not influence the pixels as much as in narrow and shallow waters. However Figure 21 shows the same pattern as in Raigastvere. Pixels are affected in the coastal areas and in the middle of the summer. It means that C2RCC is no capable to estimate ρ in the coastal areas and not only narrow lakes are influenced.

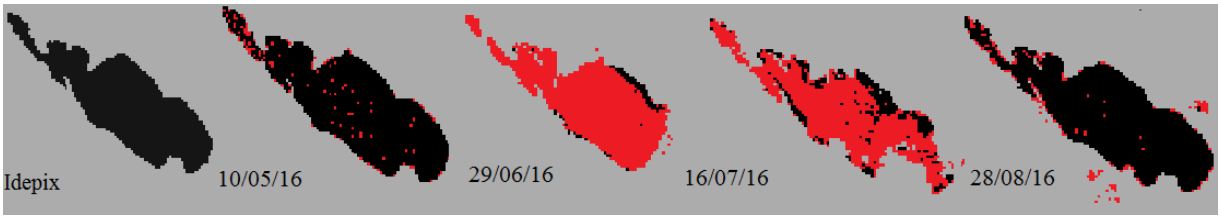

Figure 21. Time series of Saadjärv, where 'Red pixels' are showing the condition band 3 < band 1 and 'Black pixels' are representing water pixels.

3.3.2. Ecologcal status of lakes based on chl-a

For estimating ecological class based on chl-a, the specific thresholds have to be considered for each lake type (Table 2). For deriving chl-a from C2RCC, the condition band 3 > band 1 is considered to be true ρ spectrums.

Ermistu (Figure 22) and Hino (Figure 23) belong to Type 2 (non-stratified, water color dark/light), where chl-a is between 10.8-28 mg/m^3, assigns the lake into"good" status class. Ermistu has the surface area of 450 ha, width of the lake is 1.8 km and length 4 km with round shape shoreline (EELIS: Keskkonnaagentuur 2018). Hino is previously described in paragraph 3.16, with the water surface of 207 ha.

The Three-Band NIR Red Model chl-a = $65.0*((1/R_{665}-1/R_{705})*R_{740})+10.2$ and Four-Band NIR Red Model chl-a = $43.2*(1/R_{665}-1/R_{705})/(1/R_{740}-1/R_{705})+10.2$ approach worked best and showed similar trend with *in situ* measured chl-a. Standard C2RCC algorithm is estimating chl-a similarly to empirical algorithms but the range of minimum and maximum values are higher and makes it less stable for estimating chl-a (Figure 22c and Figure 23c). As these lakes are with large water surface (ha > 207 ha), the ρ of C2RCC was estimated well, because adjacency effect did not influence the water pixels of the lake. Both *in situ* and S2/MSI derived chl-a values are low (chl-a < 10 mg/m^3) (Figure 22a and Figure 23a) and there is no strong chl-a absorption peak in the C2RCC ρ spectrums (Figure 22b and Figure 23b), which is reflected in the stable seasonal dynamics. The ecological water status in Ermistu was estimated "very good" by *in situ* measurements (N = 4) and by derived chl-a (N = 10). The same water status is esimated in Hino as well by *in situ* measurements (N = 5) and by derived chl-a (N = 7).

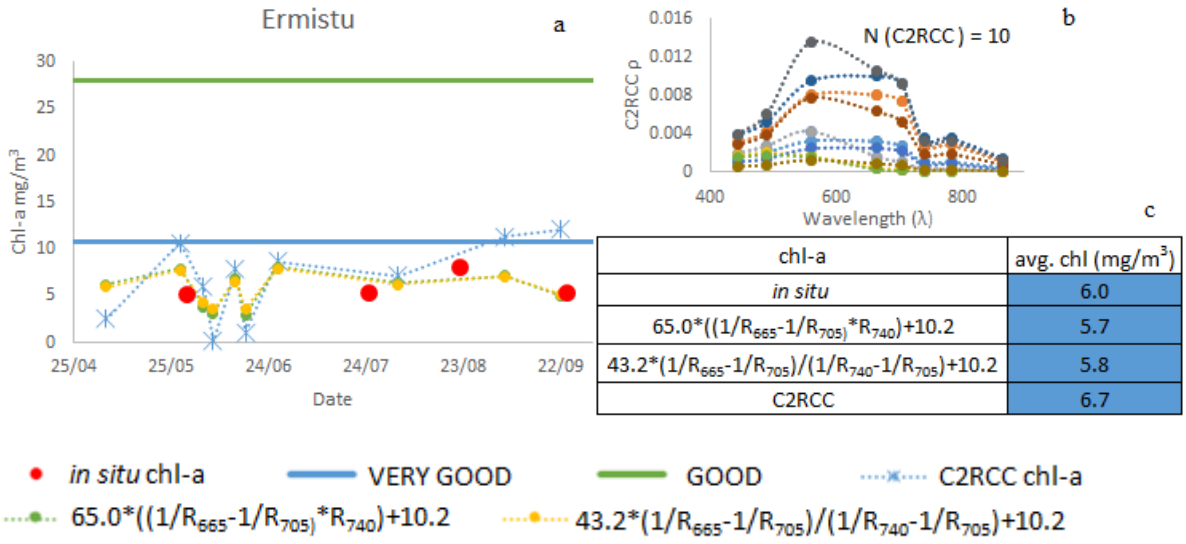

c

chl-a	avg. chl (mg/m^3)
in situ	6.0
65.0*((1/R_{665}-1/R_{705})*R_{740})+10.2	5.7
43.2*(1/R_{665}-1/R_{705})/(1/R_{740}-1/R_{705})+10.2	5.8
C2RCC	6.7

Figure 22. Estimation of chl-a seasonal dynamics in Ermistu in 2017 (a). C2RCC derived ρ (b) and vegetation period average chl-a and respective ecological status of water(c)

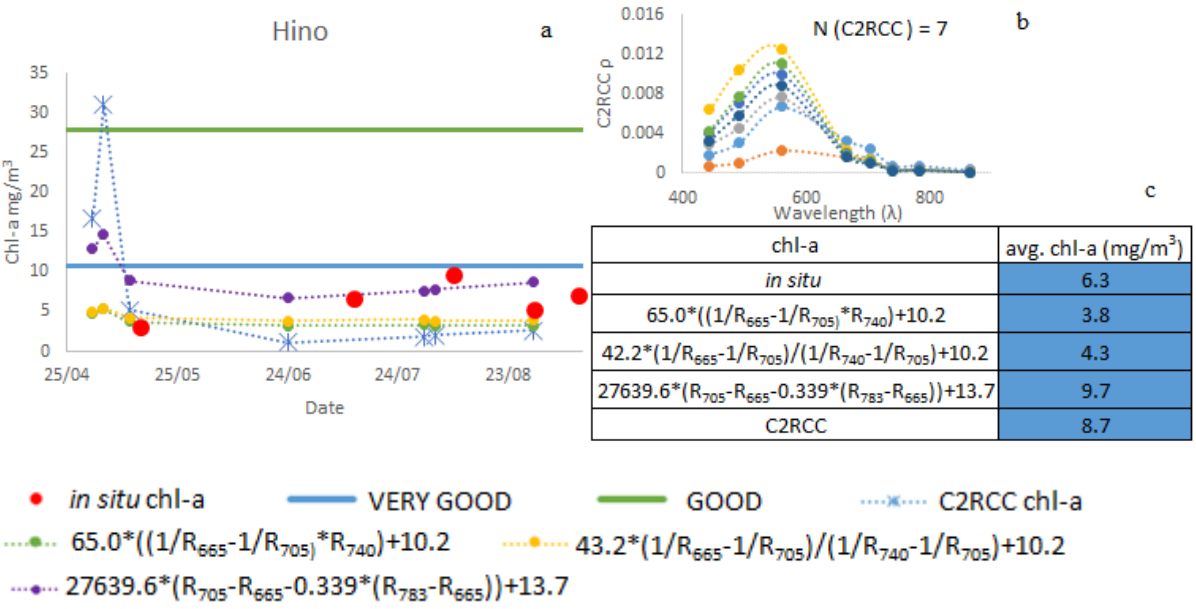

c

chl-a	avg. chl-a (mg/m^3)
in situ	6.3
65.0*((1/R_{665}-1/R_{705})*R_{740})+10.2	3.8
42.2*(1/R_{665}-1/R_{705})/(1/R_{740}-1/R_{705})+10.2	4.3
27639.6*(R_{705}-R_{665}-0.339*(R_{783}-R_{665}))+13.7	9.7
C2RCC	8.7

Figure 23. Estimation of chl-a seasonal dynamics in Hino in 2017 (a). C2RCC derived ρ (b) and vegetation period average chl-a and respective ecological status of water(c)

Pangodi (Figure 24), Pühajärv (Figure 25) and Ähijärv (Figure 26) belong to Type 3 (stratified, water color dark/light), therefore chl-a should be between 5.8-13 mg/m^3 to maintain "good" ecological water status by chl-a. Pangodi is previously described in paragraph 3.1.2, with water surface of 93.3. Pühajärv has complicated shoreline, but the

water surface is 293.3 ha and it is 1.6 km wide and 3.5 km long. Ähijärv has water surface of 183 ha with the length of 2.5 km and the width of 1 km (EELIS: Keskkonnaagentuur 2018). Empirical algorithm chl-a = 24385.4*(R_{705}-((R_{665}+R_{740})/2))+7.7 and MCI based algorithm chl-a = 27639.6*(R_{705}-R_{665}-0.339*(R_{783}-R_{665}))+13.7 give the most accurate results for these large lakes. Other investigated algorithms are not showing the dynamics of chl-a or gave negative values.

Derived chl-a values were similar to *in situ* measurements in Pangodi (chl-a = 10-12 mg/m^3) and the dynamics of chl-a changes were estimated well, where the chl-a was higher in June and in the end of the August (Figure 24a). Standard C2RCC algorithm estimated chl-a either really low or high. ρ of Pangodi was showing slight chl-a absorption peak at 675 nm, (Figure 24b) as measured from water samples. There were twice as many S2/MSI images as collected water samples (N= 8). Based on the *in situ* measurements, empirical algorithms and standard C2RCC, then ecological status of water is classified as "good"(Figure 24c).

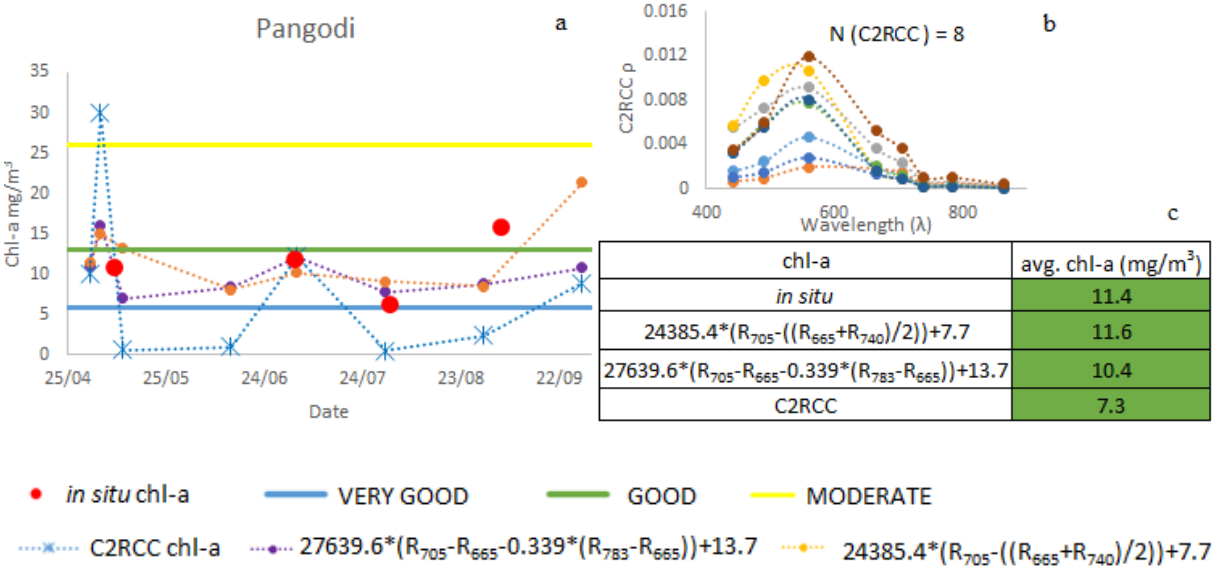

chl-a	avg. chl-a (mg/m^3)
in situ	11.4
24385.4*(R_{705}-((R_{665}+R_{740})/2))+7.7	11.6
27639.6*(R_{705}-R_{665}-0.339*(R_{783}-R_{665}))+13.7	10.4
C2RCC	7.3

Figure 24. Estimation of chl-a seasonal dynamics in Pangodi in 2017 (a). C2RCC derived ρ(b) and vegetation period average chl-a and respective ecological status of water(c).

Chl-a in Pühajärv was under 15 mg/m^3, based on the *in situ* measurements, and the dynamics of chl-a was stable. Empirical algorithms are overestimating chl-a in spring (Figure 25a), due to that they classify ecological status of water to "moderate" class (Figure 25c), whereas standard C2RCC and *in situ* measurements support "good" ecological class. Opposite to

Pühajärv, the chl-a was higher in Ähijärv and the dynamics was more varying, higher in the end of June and in the end of August (Figure 25a). ρ of Ähijärv was showing slight chl-a absorption (Figure 25b), but not as strong as it should be with chl-a over 20 mg/m^3 and that is why chl-a was underestimated by empirical algorithms in the end of June. However, empirical algorithms estimated changes as *in situ* measurements did, but standard CR2CC algorithm was giving very low or very high concentrations, which has been noticed previously. On the basis of *in situ* measurements, empirical and standard C2RCC algorithms, the ecological water status of chl-a was classified as "moderate" The number of water samples from Pühajärv was 5 and from Ähijärv 4, whereas the number of derived chl-a was 8.

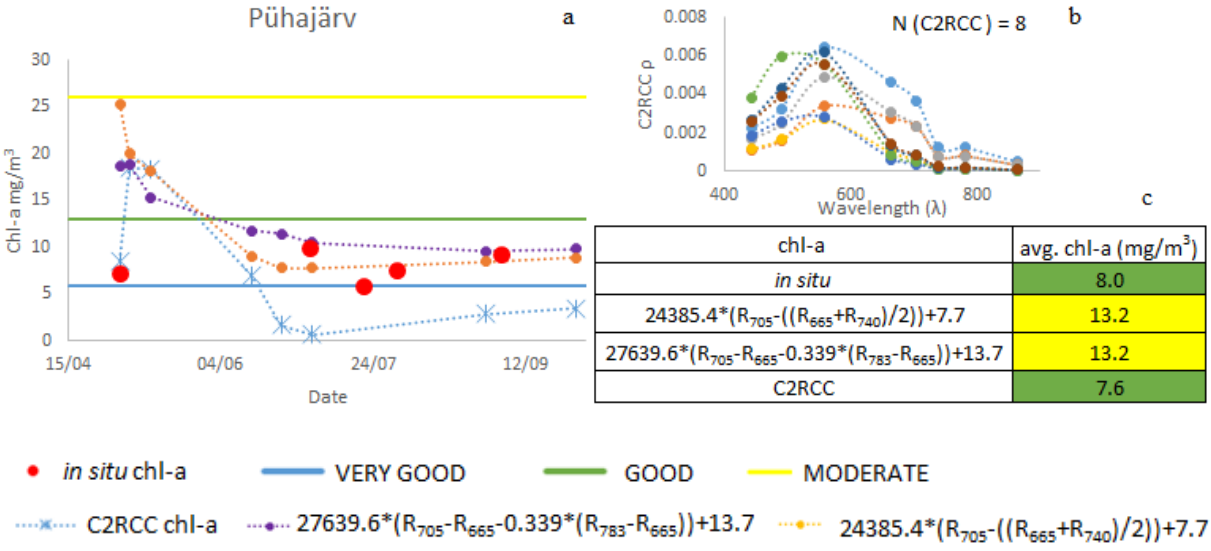

chl-a	avg. chl-a (mg/m^3)
in situ	8.0
24385.4*(R_{705}-((R_{665}+R_{740})/2))+7.7	13.2
27639.6*(R_{705}-R_{665}-0.339*(R_{783}-R_{665}))+13.7	13.2
C2RCC	7.6

Figure 25. Estimation of chl-a seasonal dynamics in Pühajärv in 2017 (a). C2RCC derived ρ (b) and vegetation period average chl-a and respective ecological status of water(c).

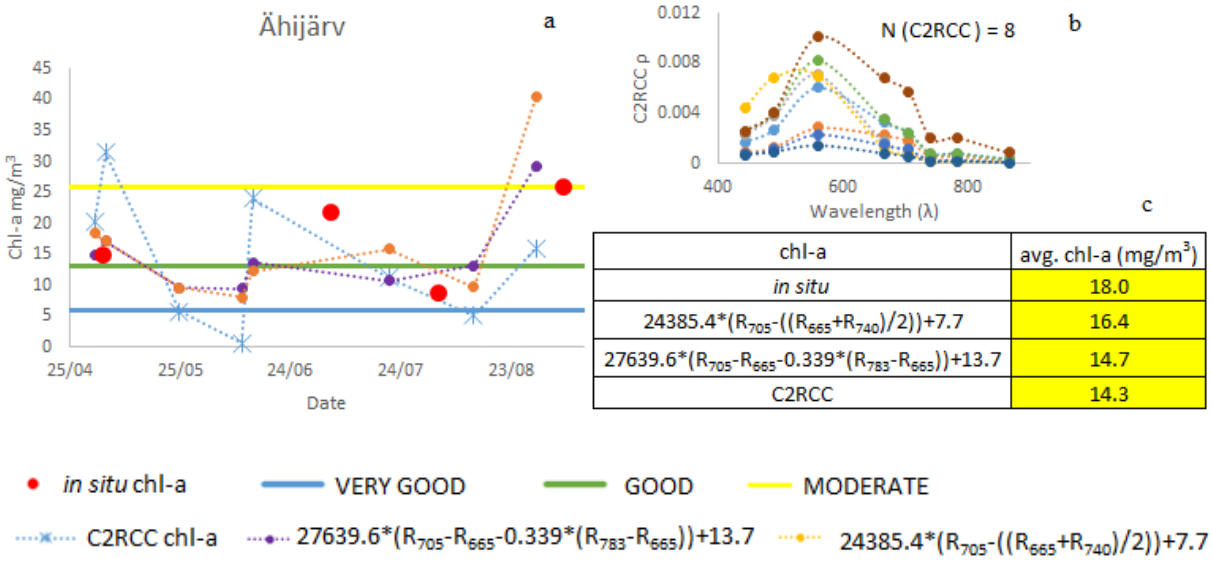

chl-a	avg. chl-a (mg/m^3)
in situ	18.0
24385.4*(R_{705}-((R_{665}+R_{740})/2))+7.7	16.4
27639.6*(R_{705}-R_{665}-0.339*(R_{783}-R_{665}))+13.7	14.7
C2RCC	14.3

Figure 26. Estimation of chl-a seasonal dynamics in Ähijärv in 2017 (a). C2RCC derived ρ (b) and vegetation period average chl-a and respective ecological status of water(c).

Pulli (Figure 27), with water surface of 63 ha and the length of 1.1 km and witdh of 0.7 m (EELIS: Keskkonnaagentuur 2018), belongs to Type 5 (non-stratified, water color light), where ecological water status "good" is assigned with chl-a 5.4-13 mg/m^3.

MCI based empirical algorithm chl-a = 27639.6*(R_{705}-R665-0.339*(R_{783}-R_{665})) +13.7 gave similar chl-a as *in situ* measuremetns increasing from July to August (Figure 27a). Most of the cases empirical algorithms underestimated *in situ* measurements strongly similar to standard C2RCC. As the chl-a levels were high (> 15 mg/m^3), then slight chl-a absorption on the ρ was detected (Figure 27b), but not as strong as it should have be. As the water surface of Pulli is small, then C2RCC was still estimating ρ as Case 2 spectrums (Figure 27c). The shape of the Pulli is round, which could change the lake suitable for C2RCC, because of smaller adjacency effect. MCI based algorithm estimated ecological water status of chl to "moderate", similarly to *in situ* measurements, but it was based only on 3 chl-a water samples, whereas number of derived chl-a was 7.

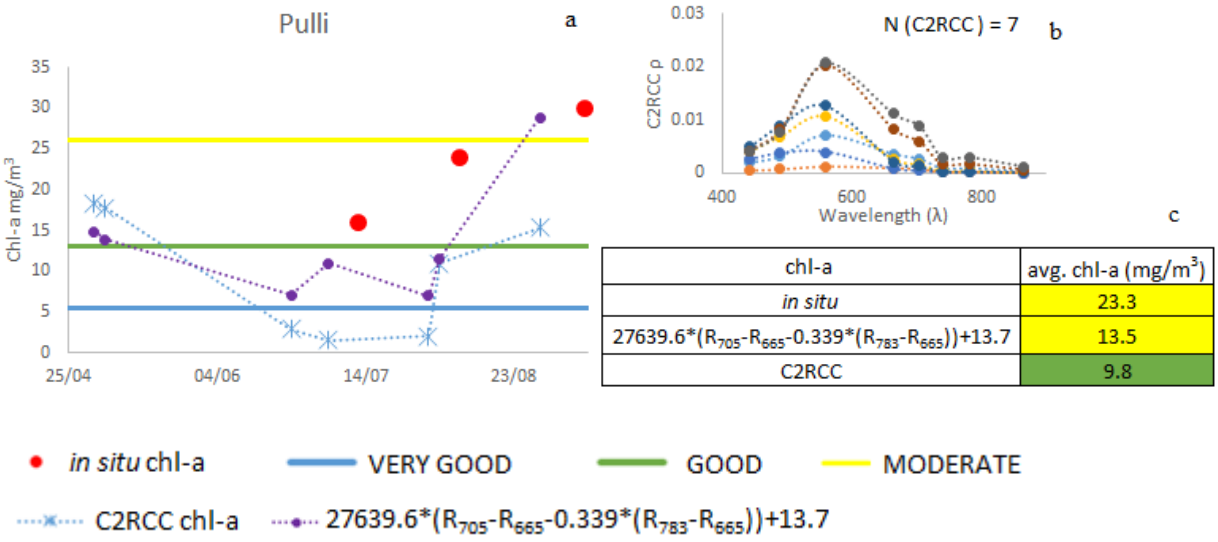

chl-a	avg. chl-a (mg/m^3)
in situ	23.3
27639.6*(R_{705}-R_{665}-0.339*(R_{783}-R_{665}))+13.7	13.5
C2RCC	9.8

Figure 27. Estimation of chl-a seasonal dynamics in Pulli in 2017 (a). C2RCC derived ρ (b) and vegetation period average chl-a and respective ecological status of water (c).

Peipsi 2 (Figure 28) and Peipsi 4 (Figure 29) belong to Type 6 and were described previously in paragraph 3.1.3. The chl-a was classified "good", where chl-a remain between 3-8 mg/m^3. Three-Band NIR Red Model algorithm chl-a = 260.1*((1/R_{665}-1/R_{705})*R_{740})+27.9, with different coeffcients for in Type 2 lakes, and MCI based algorithm gave similar dynamics of chl-a (Figure 28a and Figure 29a). MCI based algorithm overestimated the values during the summer, but estimated the shape of the *in situ* ρ spectrum well. Three-Band NIR Red Model algorithm and standard C2RCC underestimates *in si*tu measurements at some point, however showed dynamics of chl-a. As Peipsi is larger lake, then water pixels were not affected as much as for small lakes from coastline, which were showed by the number of suitable C2RCC pixels (N = 13). Based on the *in situ* measurements, Peipsi 2 and Peipsi 4 were classified as "moderate" ecological water status (Figure 28c and Figure 29c). As MCI based algorithm overestimated *in situ* measurements, then it classified Peipsi 4 in "bad" class.

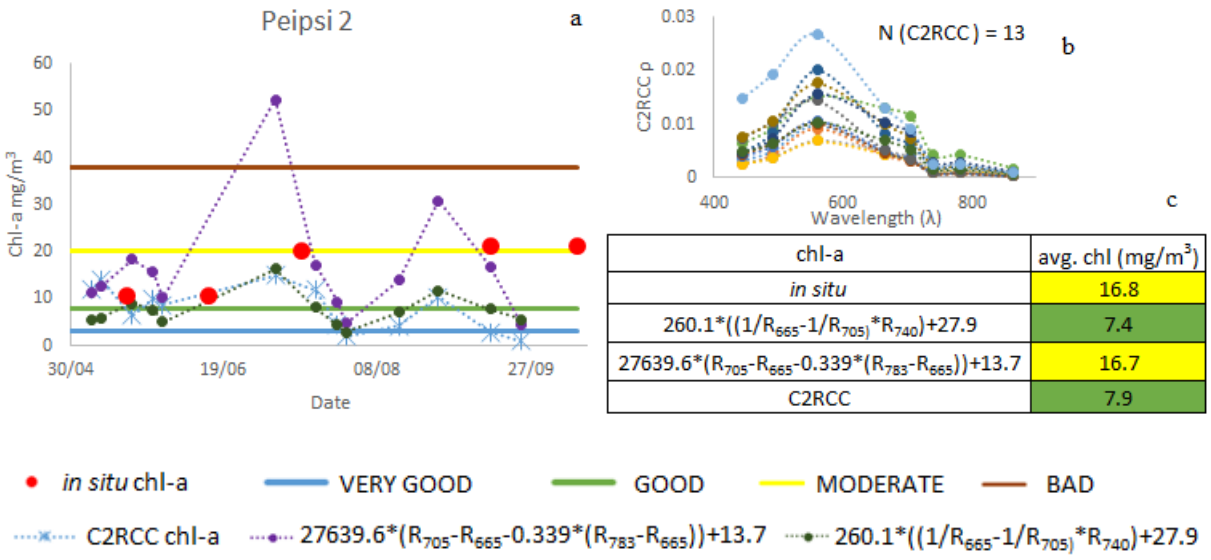

chl-a	avg. chl (mg/m³)
in situ	16.8
260.1*((1/R_{665}-1/R_{705})*R_{740})+27.9	7.4
27639.6*(R_{705}-R_{665}-0.339*(R_{783}-R_{665}))+13.7	16.7
C2RCC	7.9

Figure 28. Estimation of chl-a seasonal dynamics in point Peipsi 2 in 2016 (a). C2RCC derived ρ (b) and vegetation period average chl-a and respective ecological status of water(c).

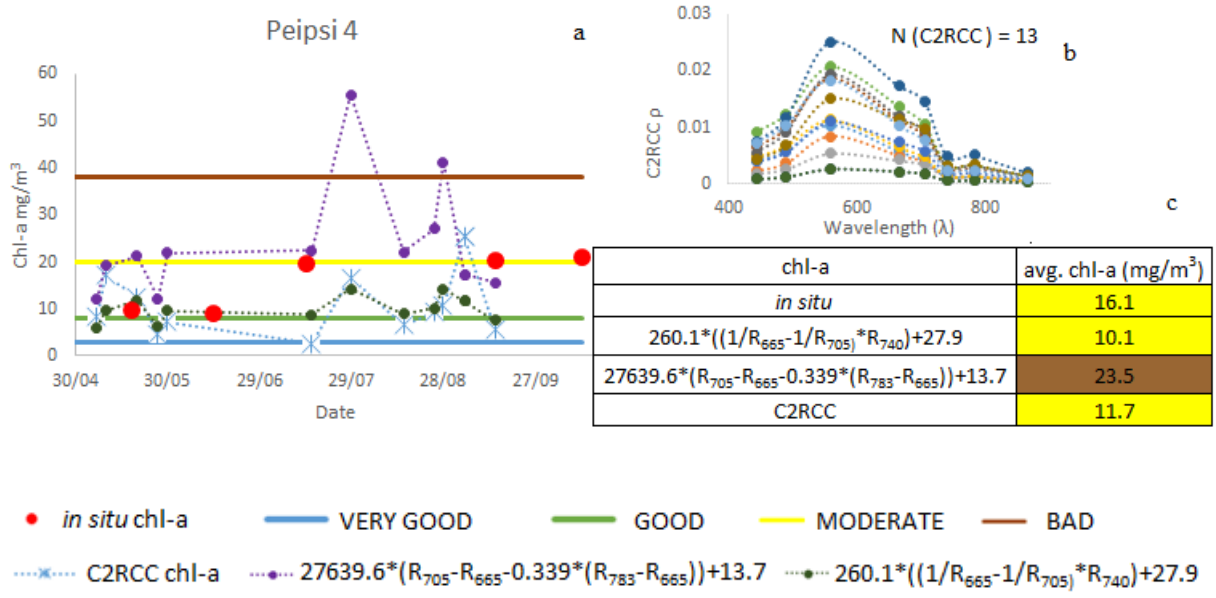

chl-a	avg. chl-a (mg/m³)
in situ	16.1
260.1*((1/R_{665}-1/R_{705})*R_{740})+27.9	10.1
27639.6*(R_{705}-R_{665}-0.339*(R_{783}-R_{665}))+13.7	23.5
C2RCC	11.7

Figure 29. Estimation of chl-a seasonal dynamics in point Peipsi 4 in 2016 (a). C2RCC derived ρ (b) and vegetation period average chl-a and respective ecological status of water(c).

It was possible to estimate ecological water status of chl-a in some cases. The possibility of estimating chl-a depended on the capability of C2RCC to derive accurate ρ in small lakes and in the vicinity of land. In Type 2, algorithms such as chl-a = 65.0*((1/R_{665}-1/R_{705})*R_{740})+10.2 and chl-a = 3.2*(1/R_{665}-1/R_{705})/(1/R_{740}-1/R_{705})+10.2 worked well,

giving similar results as *in situ* measurements. Modified MCI algorithm chl-a = $27639.6*(R_{705}-R_{665}-0.339*(R_{783}-R_{665}))+13.7$ adjusted to MSI bands worked well in Type 3, Type 5 and Type 7 lakes. It overestimated in same cases, but overall it worked well in Case 2 waters. Three-Band NIR-Red Model algorithm chl-a = $R_{705}-((R_{665}+R_{740})/2)$, also worked in Peipsi and smaller lakes. However standard C2RCC algorithm typically underestimated *in situ* measurements and did not give as accurate results as empirical algorithms.

As condition band 3 < band 1 was considered not the be true ρ spectrums, each lake pixel, allowing this condition, was investigated further. According to Table 13, these spectrums appear more in May and in July. Waters were dominated by phytoplankton in these months, in May after the ice melting from water surface and in July when water temperature achieve good conditions for phytoplankton blooms.

Table 13. Date of the pixels, where condition band 3 < band 1were true. Green color is representing May and yellow is representing July.

Date	Name of the lake
12/05/17	Pulli
12/05/17	Ähijärv
22/05/17	Pühajärv
22/05/17	Ähijärv
04/06/17	Pühajärv
14/07/17	Ermistu
16/07/16	P2
21/07/17	Hino
24/07/17	Ermistu
24/07/17	Pühajärv
24/07/17	Pulli
19/09/17	Pangodi
29/09/17	Ähijärv

SUMMARY

The EU WFD obligate to monitor larger than 50 ha lakes and derive its ecological status. The goal is to achieve at least "good" ecological status and take measures to improve the status, if needed. S2/MSI has suitable spatial resolution 10, 20, 60 m, which could support developing new applications in lakes for fulfilling WFD monitoring requirements. With both satellites, S2A and S2B, the temporal resolution is 2-3 days, which gives the possibility to analyze more data for testing and developing new applications for S2/MSI satellites. Even more, it gives the advantages to provide time series and dynamics of chl-a in lakes and coastal areas.

S2/MSI is meant for vegetation, therefore it is important to compare different AC processors for finding out the best for water As AC is essential tool for developing chl-a algorithms, four different AC processors: ACOLITE, C2RCC, Polymer and Sen2Cor were tested in this study. As the main purpose of the study was to find the best AC processor for Estonian small lakes, then based on the 6 days match-ups, C2RCC were chosen due to the high correlation with *in situ* measurements at bands useable for deriving chl-a.

As chl-a is one of the main parameter for estimating ecological status of water based on WFD, the second part of the study included testing and developing chl-a algorithms adjusted to S2/MSI bands. As S2/MSI band (665 nm) near the chl-a absorption peak is wider (38 nm) than S3/OLCI's (7.5 nm), then comparison of chl-a absorption bands were conducted, which showed that, S2/MSI is capable to detect chl-a over large range of values. Further investigation showed that C2RCC is not able to give accurate results in small, narrow lakes, where adjacency effect affects the pixels near the coastline.

Therefore, it is important to develop corrections for adjacency effect, which could help to avoid invalid mixed pixels from analyses. In shallow lakes, bottom effect could also influence pixels near shore and produce errors in signal due to the bottom reflectance. As AC is very important procedure, AC processors are tested and developed continuously to provide best quality for Level 2 data, needed for the development of new applications.

In some cases, where adjacency effect is smaller, especially in larger lakes (over 90 ha) and where the shape of the lake is round, it is possible to estimate chl-a in water surface using empirical algorithms. Standard C2RCC chl-a algorithm constantly estimates the value of chl-a either high or low, compared to *in situ* data, but with similar seasonal dynamics. MCI based algorithm showed good results in high chl-a lakes, with Three-Band NIR Red Model algorithm $(1/R_{665}-1/R_{705})*R_{740}$ and $R_{705}-((R_{665}+R_{740})/2)$ algorithm. In the lakes with low chl-a and high TSM concentration, Four-Band NIR Red model algorithm $(1/R_{665}-1/R_{705})/(1/R_{740}-1/R_{705})$ worked best, removing TSM influence, and previously named Three-Band NIR Red Model algorithm.

Furthermore, C2RCC processor was not very sensitive to estimate chl-a absorption at band 665 nm, because the chl-absorption peak is not very detectable from ρ due to the adjacency effect in small lakes. It means that more validation data from optically complex waters are essential for improving AC processors. However, the number of derived chl-a is twice as high as *in situ* measurements, which give advantage to collect twice as much data from lakes.

S2/MSI has potential for deriving water quality parameters from small lakes for fulfilling EU WFD monitoring and reporting requirements. Improvements of ACs are essential for using S2/MSI advantages over *in situ* measurements and support the regular monitoring in small lakes.

KOKKUVÕTE

EL veepoliitika raamdirektiiv kohustab seirata järvi, mille suurus on vähemalt 50 ha ja hinnata nende ökoloogilist seisundit. Eesmärgiks on saavutada vee ökoloogiline seisund vähemalt "hea", vajadusel rakendada meetmeprogramme selle saavutamiseks. S2/MSI-l on sobiv ruumiline lahutus 10, 20, 60 m, mis võimaldab uute rakenduste arendamist järvedes, et täita EL veepoliitika raamdirektiivi nõudeid. Mõlema satelliidi, S2A ja S2B, korral on ajaline lahutus kesklaiustel 2-3 päeva, mis annab võimaluse analüüsida rohkem andmeid, et testida ja arendada uusi rakendusi S2/MSI satelliitidele. Veelgi enam, suur ajaline lahutus annab võimaluse koostada aegridu ja hinnata chl-a dünaamikat järvedes ja rannikualadel.

S2/MSI on taimkatte kaugseire satelliit, mistõttu on oluline võrrelda erinevaid atmosfäärikorrektsiooni protsessoreid, et leida parim vee kaugseireks. Kuna edukas atmosfäärikorrektsioon on oluline eeldus chl-a algoritmide arendamisel, siis töö käigus testiti nelja erinevat atmosfäärikorrektsiooni: ACOLITE, C2RCC, Polymer ja Sen2Cor. Töö üheks eesmärgiks oli leida parim atmosfäärikorrektsioon, siis põhinedes 6-le kontaktmõõtmiste ja satelliidiandmete võrdlusele, osutus valituks C2RCC, millel oli kõige kõrgem vee peegeldusteguri korrelatsioon põhilistel chl-a algoritmi arendamise kanalitel võrreldes *in situ* vee peegeldusteguriga.

Chl-a on põhiline parameeter vee ökoloogilise seisundiklassi hindamisel, seetõttu teine osa uurimistööst hõlmas chl-a algoritmide testimist ja arendamist S2/MSI kanalite jaoks. Kuna S2/MSI kanal (665 nm) chl-a neeldumispiigi lähedal on laiem (38 nm) kui S3/OLCI (7.5 nm) kanal, siis uurimistöö käigus viidi läbi võrdlus chl-a kanalite vahel, mis näitas, et S2/MSI on võimeline tuvastama chl-a erinevate kontsentratsioonide korral.. Edasine uurimine selgitas, et C2RCC ei ole võimeline andma täpseid tulemusi väikeste, kitsaste järvede korral, kus naabrusefekt mõjutab kaldaäärseid piksleid. Seetõttu on väga oluline arendada korrektsioone ka naabrusefekti eemaldamise jaoks, mis aitaksid vältida segupiksleid. Madalates järvedes, mängib olulist rolli ka põhjaefekt, mis mõjutab piksleid kaldaäärsetes alades ja segab vee peegeldustegurit põhjast tuleva peegeldusega. Kuna atmosfäärikorrektsioon on väga tähtis protseduur, siis käib pidev algoritmide testimine ja arendamine, et tagada parim Level-2 piltide informatsioon, et oleks võimalik arendada välja uusi rakendusi.

Mõnedel juhtudel, kus naabrusefekt on väiksem, eriti suuremates järvedes (üle 90 ha) ja kus järv on ümmargune, seal on võimalik hinnata chl-a vees, kasutades empiirilisi algoritme. Standard C2RCC algoritm hindas järjepidevalt chl-a, kas liiga kõrgeks või liiga madalaks, kuid siiski säilitas chl-a dünaamika sarnaselt *in situ* mõõtmistega. MCI-l põhinev algoritm näitas häid tulemusi kõrge chl-a järvedes, koos Three-Band NIR Red Model $(1/R_{665}-1/R_{705})*R_{740}$ ja $R_{705} - ((R_{665} + R_{740})/2)$ algoritmiga. Madala chl-a ja kõrge TSM sisaldusega järvedes töötas hästi Four-Band NIR Red Model algoritm $(1/R_{665}-1/R_{705})/(1/R_{740}-1/R_{705})$, mis eemaldab TSM segava mõju, ning lisaks eelnevalt nimetatud Three-Band NIR Red Model algoritm.

Veelgi enam, atmosfäärikorrektsioon C2RCC ei ole väga tundlik hindamaks chl-a neeldumist 665 nm kanali juures, sest chl-a neeldumispiik ei ole väga hästi näha vee peegeldustegurilt tänu naabrusefektile väikestes järvede. See tähendab, et vajalikud on valideerimisandmed optiliselt keerukatest järvedest, et arendada atmosfäärikorrektsioone. Siiski on satelliidi andmetelt saadud chl-a arv kaks korda suurem kui *in situ* mõõtmistelt saadud arv, mis annab võimaluse koguda kaks korda rohkem andmeid järvedest.

S2/MSI-l on palju eeliseid, et tuletada veekvaliteedi parameetreid väikejärvedel, et täita EU veepoliitika raamdirektiivi. Atmosfäärikorrektsioonide parandused ja täiustused on väga vajalikud, et oleks võimalik kasutada S2/MSI eeliseid *in situ* mõõtmiste ees ja tagada regulaarne seire väikejärvedes.

Acknowledgements

I would like to thank you my supervisor Krista Alikas, who has been ready for answering all my questions and helping me out with different problems. She has been supporting me, for obtaining as may knowledges as possible for conducting this study and giving constructive feedback during the two years.

I would also like to thank you Tartu Observatory water remote sensing work group, who has performed fieldworks for collecting water-leaving reflectance *in situ* measurements and gathered data in the Tartu Observatory database. Furthermore, they are supporting me and help me with their knowledges. This research has received funding from the European Union's Horizon 2020 research and innovation programme (grant agreement n° 730066) and Estonian Research Council grant PSG10. Especially I thank you Kristi Uudeberg helping me with programming.

In addition, I would like to thank personnel in the Center for Limnology for fieldwork and laboratory measurements. Without them developing and validating chl-a algorithms would not be possible.

I would like to thank you all the people who supported me and helped me during conducting this study.

References

1. Alikas, K., Kangro, K., Randoja, R., Philipson, P., Asuküll, E., Pisek, J., Reinart, A. (2015), "Satellite-based products for monitoring optically complex inland waters in support of EU Water Framework Directive," International Journal of Remote Sensing, **36** (17), 4446-4468.
2. Alikas, K. (2016), "From research to applications: monitoring optically complex waters with MERIS/ENVISAT data," PhD thesis, University of Tartu.
3. Baillarin, S. J., Meygret, A., Dechoz, C., Petrucci, B., Lacherade, S., Tremas, T., Isola, C., Martimort, P., Spoto, F. (2012), "Sentinel-2 Level 1 products and image processing performances," Archives of the Photogrammetry, Remote Sensing and Spatial Information Sciences, **39**-B1, 2012 XXII ISPRS Congress, 25 August – 01 September 2012, Melbourne, Australia.
4. Brockmann, C., Roland, D., Marco, P., Stelzer, K., Sabine, E., Ana, R. (2016), "Evolution of the C2RCC Neural Network for Sentinel 2 and 3 for the retrieval of ocean colour products in normal and extreme optically complex waters," Proc. 'Living Planet Symposium 2016', Prague, Czech Republic, 9–13 May 2016 (ESA SP-740, August 2016)
5. Candiani, G., Giardino, C., Brando, V. E. (2007), "Adjacency effects and bio-optical model regionalisation: MERIS data to assess lake water quality in the subalpine ecoregion," Proc. 'Envisat Symposium 2007', Montreux, Switzerland 23–27 April 2007 (ESA SP-636, July 2007).
6. Chavula, G., Brezonik, P., Thenkabail, P., Johnson, T., Bauer, M. (2009), "Estimating chlorophyll concentration in Lake Malawi from MODIS satellite imagery," Physics and Chemistry of the Earth, **34**, 755–760.
7. Chen, Q., Zhang, Y., Ekroos, A., Hallikainen, M. (2004), "The role of remote sensing technology in the EU water framework directive (WFD)," Environmental Science & Policy, **7** (4**)**, 267–276.
8. Chen, Q., Zhang, Y., Hallikainen, M. (2007), "Water quality monitoring using remote sensing in support of the EU water framework directive (WFD): A case study in the Gulf of Finland," Environmental Monitoring and Assessment, **124**, 157–166.

9. Dörnhöfer, K., Klinger, P., Heege, T., Oppelt, N. (2018), "Multi-sensor satellite and in situ monitoring of phytoplankton development in a eutrophic-mesotrophic lake," Science of the Total Environment, **612**, 1200–1214.
10. Dörnhöfer, K., Oppelt, N. (2016), "Remote sensing for lake research and monitoring – Recent advances," Ecological Indicators, **64**, 105–122.
11. Duan, H., Zhang, Y., Zhang, B., Song, K., Wang, Z. (2007), "Assessment of Chlorophyll-a Concentration and Trophic State for Lake Chagan Using Landsat TM and Field Spectral Data," Environmental Monitoring and Assessment, **129**, 295–308.
12. EELIS (Eesti Looduse Infosüsteem - Keskkonnaregister): Keskkonnaagentuur. Accessed 10.05.2018: http://loodus.keskkonnainfo.ee/eelis/
13. Eesti Maaülikooli põllumajandus- ja keskkonnainstituut (2016), "Eesti väikejärvede hüdrobioloogiline seire 2016.a," aruanne, Tartu.
14. European Commission (2000). Directive of the European Parliament and of the Council 2000/60/EC, establishing a framework for community action in the field of water policy
15. Ferreira, J. G., Vale, C., Soares, C. V., Salas, F., Stacey, P. E., Bricker, S. B., Silva, M. C., Marques, J. C. (2007), ,"Monitoring of coastal and transitional waters under the E.U. Water Framework Directive," Environmental Monitoring and Assessment, **135**. 195–216.
16. Gitelson, A. (1992), "The Peak near 700 nm on radiance spectra of algae and water relationships of its magnitude and position with chlorophyll concentration," Int. J. Remote Sensing, **13**, 3367–3373.
17. Gitelson, A.A., Gritz, Y., Merzlyak, M.N. (2003), "Relationships between leaf chlorophyll content and spectral reflectance and algorithms for non-destructive chlorophyll assessment in higher plant leaves," Journal of Plant Physiology, **160**, 271–282.
18. Gower, J. F. R., Doerffer, R., Borstad, G. A. (1999), "Interpretation of the 685nm peak in waterleaving radiance spectra in terms of fluorescence, absorption and scattering, and its observation by MERIS," Int. J. Remote Sensing, **20** (9), 1771-1786.
19. Gower, J., King, S., Goncalves, P. (2008), "Global monitoring of plankton blooms using MERIS MCI," International Journal of Remote Sensing, **29** (21), 6209–6216

20. IOCCG (2000), “Remote Sensing of Ocean Colour in Coastal, and Other Optically-Complex, Waters,” Sathyendranath, S. (ed.), Reports of the International Ocean-Colour Coordinating Group, No. 3, IOCCG, Dartmouth, Canada.
21. Jeffrey, S. W., Humphrey, G. F. (1975), “New spectrophotometric equation for determining chlorophyll a, b, c1 and c2,” Biochemie und Physiologie der Pflanzen, **167** (2), 194-204.
22. Krebs, G. D. (2017), “Sentinel 2A, 2B, 2C, 2D,” Accessed 10.05.2018: http://space.skyrocket.de/doc_sdat/sentinel-2.htm
23. Klein. T., Nilsson, M., Persson, A., Håkansson, B. (2017), “From Open Data to Open Analyses—New Opportunities for Environmental Applications?” Environments, **4**, 32.
24. Le, C.; Li, Y.; Zha, Y.; Sun, D.; Huang, C.; Lu, H. (2009), “A four-band semi-analytical model for estimating chlorophyll a in highly turbid lakes: The case of Taihu lake, China,” Remote Sensing Environment, **113**, 1175–1182.
25. Lins, R. C., Martinez, J., Marques, D. M., Cirilo, J. A., Fragoso Jr, C. R. (2017), “Assessment of Chlorophyll-a Remote Sensing Algorithms in a Productive Tropical Estuarine-Lagoon System,” Remote Sensing, **9**, 516.
26. Maa-ameti kaardiserver: aluskaart (2018)
27. Malenovsky, Z., Rott, H., Cihlar, J., Schaepman, M. E., Garcia-Santos, G., Fernandes, R., Berger, M. (2012), “Sentinels for science: Potential of Sentinel-1, -2, and -3 missions for scientific observations of ocean, cryosphere, and land,” Remote Sensing of Environment, **120**, 91–101.
28. Mandanici, E., Bitelli, G. (2016), “Preliminary Comparison of Sentinel-2 and Landsat 8 Imagery for a Combined Use,” Remote Sensing, **8**, 1014.
29. Matthews, M. W. (2011), “A current review of empirical procedures of remote sensing in inland and near-coastal transitional waters,” International Journal of Remote Sensing, **32** (21), 6855-6899.
30. Matthews, M. W., Bernard, S., Winter, K. (2010), “Remote sensing of cyanobacteria-dominant algal blooms and water quality parameters in Zeekoevlei, a small hypertrophic lake, using MERIS,” Remote Sensing of Environment, **114**, 2070–2087.
31. Ministry of Environment, Regulations (2009). “Pinnaveekogumite moodustamise kord ja nende pinnaveekogumite nimestik, mille seisundiklass tuleb määrata, pinnaveekogumite seisundiklassid ja seisundiklassidele vastavad kvaliteedinäitajate

väärtused ning seisundiklasside määramise kord.” RTL 64, 941. Accessed 27.04.2018: https://www.riigiteataja.ee/akt/13210253

32. Mitchell, B. G., Kahru, M. (1998), “Algorithms for SeaWiFS developed with the CalCOFI data set,” CalCOFI Report, **39**, 133-159.
33. Morel, A.; Prieur, L. (1977), “Analysis of variations in ocean color1,” Limnology and Oceanography **22**, 709–722.
34. Moses, W. J., Gitelson, A. A., Berdnikov, S., Povazhnyy, V. (2009), “Estimation of chlorophyll-a concentration in case II waters using MODIS and MERIS data—successes and challenges,” Environmental Research Letters, **4**, 045005.
35. Munne, A., Prat, N. (2006), “Ecological aspects of the Water Framework Directive,” The Water Framework Directive in Catalonia, 53-75.
36. Mäemets, A. (1997), “Eesti NSV järved ja nende kaitse,” Tallinn: Valgus, lk 262.
37. Müller-Wilm, U., Louis, J., Richter, R., Gascon, F., Niezette, M. (2013), “Level 2A prototype processor: Architecture, algorithms and first results,” Proc. ‘ESA Living Planet Symposium 2013’, Edinburgh, UK 9–13 September 2013 (ESA SP-722, December 2013).
38. Odermatt, D., Gitelson, A., Brando, V. E., Schaepman, M. (2012), “Review of constituent retrieval in optically deep and complex waters from satellite imagery,” Remote Sensing of Environment, **118**, 116–126.
39. O’Reilly, J. E., Maritorena, S., Mitchell, B. G., Siegel, D. A., Carder, K. L., Garver, S. A., Kahru, M., McClain, C. (1998), “Ocean color chlorophyll algorithms for SeaWiFS,” Journal of Geophysical Research, **103**, 24937-24953
40. Pahlevan, N., Sarkar, S., Franz, B. A., Balasubramanian, S. V., He, J. (2017), “Sentinel-2 MultiSpectral Instrument (MSI) data processing for aquatic science applications: Demonstrations and validations.” Remote Sensing of Environment, **201**, 47–56.
41. Qin, P., Simis, S. G. H., Tilstone, G. H. (2017), “Radiometric validation of atmospheric correction for MERIS in the Baltic Sea based on continuous observations from ships and AERONET-OC,” Remote Sensing of Environment, **200**, 263–280.
42. Ruddick, K.G., De Cauwer, V., Park, Y.-J., Moore, G. (2006), “Seaborne measurements of near infrared water-leaving reflectance: The similarity spectrum for turbid waters,” Limnology and Oceanography, **51** (2), 1167–1179.

43. Salem, S. I., Higa, H., Kim, H., Kobayashi, H., Oki, K., Oki, T. (2017b), "Assessment of Chlorophyll-a Algorithms Considering Different Trophic Statuses and Optimal Bands," Sensors, **17**, 1746.
44. Salem, S. I., Strand, M. H., Higa, H., Kim, H., Kazuhiro, K., Oki, K., Oki, T. (2017a), "Evaluation of MERIS Chlorophyll-a Retrieval Processors in a Complex Turbid Lake Kasumigaura over a 10-Year Mission," Remote Sensing, **9**, 1022.
45. Stercky, S., Knaeps, E., Ruddick, K. (2011), "Detection and correction of adjacency effects in hyperspectral airborne data of coastal and inland waters: the use of the near infrared similarity spectrum," International Journal of Remote Sensing, **32** (21), 6479-6505
46. Shanmugam, P. (2012), "CAAS: an atmospheric correction algorithm for the remote sensing of complex waters," Annales Geophysicae., **30**, 203–220.
47. Steinmetz, F., Deschamps, P.-Y., Ramon, D. (2011) "Atmospheric correction in presence of sun glint: application to MERIS," Optics Express, **19** (10), 9783.
48. Tilstone, G. H., Moore, G. F., Sørensen, K., Doerffer, R., Røttgers, R., Ruddick, K. G., Pasterkamp, R., Jørgensen, P. V. (2002), "REVAMP - Regional Validation of MERIS Chlorophyll products in North Sea coastal waters," Development of Generic Earth Observation Technologies, contract: EVG1 – CT – 2001 – 00049.
49. Toming, K., Kutser, T., Laas, A., Sepp, M., Paavel, B., Nõges, T. (2016), "First experience in mapping lake water quality parameters with Sentinel-2 MSI imagery," Remote Sensing, **8**, 640
50. TÜ Eesti Mereinstituut (2013), "Veekvaliteedi hindamissüsteemi parandamine rannikuvee tüüpaladel II (Pärnu laht) ja V (Väinameri)," aruanne, Tallinn.
51. Uudeberg, K., Alikas, K., Kangro, K., Asuküll, E., Ligi, M., Ansko, I. (2014), "Tartu Observatory fieldwork methods."
52. Vanhellemont, Q., Ruddick, K. (2016), "Acolite for Sentinel-2: aquatic applications of MSI imagery. Proc. ESA Living Planet Symposium, Pragur 2016, Czech Republic, 9–13 May 2016 (ESA SP-740).
53. Werdell, P. J., McKinna, L. I. W., Boss, E., Ackleson, S. G., Craig, S. E., Gregg. W. W., Lee, Z., Maritorena, S., Roesler, C. S., Rousseaux, C. S., Stramski, D., Sullivan, J. M., Twardowski, M. M., Tzortziou, M., Zhang, X. (2018), "An overview of approaches and challenges for retrieving marine inherent optical properties from ocean color remote sensing," Progress in Oceanography, **160**, 186-212.

54. Woerd, H. J., Wernand, M. R. (2015), "True Colour Classification of Natural Waters with Medium-Spectral Resolution Satellites: SeaWiFS, MODIS, MERIS and OLCI," Sensors, **15**, 25663-25680.
55. Wozniak, M., Bradtke, K. K., Krezel, A. (2014), "Comparison of satellite chlorophyll a algorithms for the Baltic Sea," Journal of Applied Remote Sensing, **8**, 083605.
56. Yoder, J. A., McClain, C. R., Blanton, J., Oey, L-Y. (1987), "Spatial scales in CZCS-chlorophyll imagery of the southeastern U.S. continental shelf," Limnology and Oceanography, **32** (4), 929-941.
57. Zhang, F., Li, J., Shen, Q., Zhang, B., *Senior Member, IEEE*, Wu, C., Wu, Y., Wang, G., Wang, S., Lu, Z. (2015), "Algorithms and Schemes for Chlorophyll a Estimation by Remote Sensing and Optical Classification for Turbid Lake Taihu, China," IEEE Journal of Selected Topics in Applied Earth Observations and Remote Sensing, **8** (1), 350-364.
58. Zhang, Y., Ma, R., Duan, H., Loiselle, S., Xu, J. (2014), "A Spectral Decomposition Algorithm for Estimating Chlorophyll-a Concentrations in Lake Taihu, China," Remote Sensing, **6**, 5090-5106.
59. Zimba, P. V., Gitelson, A. (2006), "Remote estimation of chlorophyll concentration in hyper-eutrophic aquatic systems: Model tuning and accuracy optimization," Aquaculture **256**, 272–286.

Lihtlitsents lõputöö reprodutseerimiseks ja lõputöö üldsusele kättesaadavaks tegemiseks

Mina, Ave Ansper,

annan Tartu Ülikoolile tasuta loa (lihtlitsentsi) enda loodud teose

„Sentinel-2/MSI applications for European Union Water Framework Directive reporting purposes“,

mille juhendajateks on PhD Krista Alikas (TO, TÜ), PhD Piia Post (TÜ),

reprodutseerimiseks säilitamise ja üldsusele kättesaadavaks tegemise eesmärgil, sealhulgas digitaalarhiivi DSpace-is lisamise eesmärgil kuni autoriõiguse kehtivuse tähtaja lõppemiseni;
üldsusele kättesaadavaks tegemiseks Tartu Ülikooli veebikeskkonna kaudu, sealhulgas digitaalarhiivi DSpace´i kaudu kuni autoriõiguse kehtivuse tähtaja lõppemiseni.

olen teadlik, et punktis 1 nimetatud õigused jäävad alles ka autorile.

kinnitan, et lihtlitsentsi andmisega ei rikuta teiste isikute intellektuaalomandi ega isikuandmete kaitse seadusest tulenevaid õigusi.

Tartus, 30.05.18